Published for SISSA by Springer

Received: *April 28, 2015*
Accepted: *June 17, 2015*
Published: *July 10, 2015*

Inclusive, prompt and non-prompt J/ψ production at mid-rapidity in Pb-Pb collisions at $\sqrt{s_{\rm NN}} = 2.76$ TeV

The ALICE collaboration

E-mail: ALICE-publications@cern.ch

Abstract: The transverse momentum ($p_{\rm T}$) dependence of the nuclear modification factor $R_{\rm AA}$ and the centrality dependence of the average transverse momentum $\langle p_{\rm T}\rangle$ for inclusive J/ψ have been measured with ALICE for Pb-Pb collisions at $\sqrt{s_{\rm NN}} = 2.76$ TeV in the e^+e^- decay channel at mid-rapidity ($|y| < 0.8$). The $\langle p_{\rm T}\rangle$ is significantly smaller than the one observed for pp collisions at the same centre-of-mass energy. Consistently, an increase of $R_{\rm AA}$ is observed towards low $p_{\rm T}$. These observations might be indicative of a sizable contribution of charm quark coalescence to the J/ψ production. Additionally, the fraction of non-prompt J/ψ from beauty hadron decays, $f_{\rm B}$, has been determined in the region $1.5 < p_{\rm T} < 10$ GeV/c in three centrality intervals. No significant centrality dependence of $f_{\rm B}$ is observed. Finally, the $R_{\rm AA}$ of non-prompt J/ψ is discussed and compared with model predictions. The nuclear modification in the region $4.5 < p_{\rm T} < 10$ GeV/c is found to be stronger than predicted by most models.

Keywords: Hadron-Hadron Scattering

ArXiv ePrint: 1504.07151

doi:10.1007/JHEP07(2015)051

Contents

1 Introduction

Heavy-ion collisions at high energies allow the study of strongly interacting matter under extreme conditions. Calculations based on Quantum-Chromo-Dynamics (QCD) on the lattice indicate that the hot and dense medium created in these collisions behaves like a strongly coupled Quark-Gluon Plasma (QGP) [1–4]. Heavy quarks are an important probe for the properties of this state of matter, since they are produced via hard partonic collisions at a very early stage and thus experience the complete evolution of the system. Quarkonium states, i.e. bound states of a heavy quark and anti-quark such as the J/ψ meson ($c\bar{c}$ state) are of particular interest. It was predicted that the J/ψ formation is suppressed in a QGP due to the screening of the $c\bar{c}$ potential in the presence of free colour charges [5]. Experimentally, a suppression of the inclusive J/ψ yield in heavy-ion collisions relative to the corresponding yield in pp, scaled by the number of binary nucleon-nucleon collisions, has been observed at the Super Proton Synchrotron (SPS) [6–8] and the Relativistic Heavy Ion Collider (RHIC) [9, 10]. The level of suppression was found to be similar at SPS and RHIC, despite the significantly different collision energy. More recently, the nuclear modification of J/ψ was also measured for Pb-Pb collisions at the LHC [11–13]. While at high transverse momentum ($p_{\rm T} > 4\,{\rm GeV}/c$) the suppression factor is at the same level as the one observed at RHIC in the low $p_{\rm T}$ region, a significant reduction of the suppression is measured towards lower $p_{\rm T}$. This has been interpreted as the effect of an additional contribution to J/ψ production at low $p_{\rm T}$, due to the combination of correlated or uncorrelated c and $\bar{c}$ quarks [14, 15]. This contribution becomes sizable at LHC energies, since the number of $c\bar{c}$ pairs is much higher than at lower energies. Assuming that a deconfined phase is produced and that all the J/ψ are dissociated, this process happens at the chemical freeze-out stage of the fireball evolution. This is the approach followed within the statistical hadronization models described in refs. [16, 17]. Alternatively, J/ψ could be generated via coalescence throughout the full evolution of the QGP phase, if their survival probability in

JHEP07(2015)051

this environment is large enough. This scenario has been implemented in several partonic transport models [18, 19]. It was found that both approaches can provide a description of the measured nuclear modification factors [12] and of the elliptic flow of inclusive J/ψ [20].

The production of open beauty hadrons is expected to be sensitive to the density of the medium created in heavy-ion collisions due to the energy loss experienced by the parent parton (a beauty quark) which hadronizes into the beauty hadron. This energy loss is expected to occur via medium-induced gluon radiation [21, 22] and elastic collisional energy loss processes [23–25] and it depends on the QCD Casimir coupling factor of the parton (larger for gluons than for quarks) and on the parton mass [26–29]. Other mechanisms, such as in-medium hadron formation and dissociation, can be envisaged as particularly relevant for heavy-flavour hadrons due to their small formation times [30–32].

Inclusive J/ψ production is the sum of several contributions. In addition to the directly produced J/ψ, the decays of heavier charmonium states, such as the χ_c and ψ(2S), also contribute to the inclusive J/ψ yield. These two sources (direct and charmonium decays) are defined as prompt J/ψ, where the contribution from charmonium decays is about 35% as measured in pp collisions [33]. Since heavier charmonia are less strongly bound than the J/ψ they should be more easily dissolved in a deconfined medium [34]. The J/ψ suppression measured at the SPS is indeed compatible with the assumption that only the excited states are dissolved and not the directly produced J/ψ [6, 7]. On top of the prompt J/ψ production, there is an additional non-prompt contribution to the inclusive J/ψ at high centre-of-mass energies, coming from the decay of beauty hadrons. Since these decays proceed via weak interactions, the resulting J/ψ will originate from a decay vertex that is displaced from the main interaction vertex. Their measurement provides a direct determination of the nuclear modification of beauty hadrons. By subtracting the non-prompt contribution from the inclusive J/ψ yield one can also provide an unbiased information on medium modification of prompt charmonia. The non-prompt J/ψ contribution at mid-rapidity has already been measured in pp collisions at $\sqrt{s} = 7$ TeV by ATLAS [35], CMS [36] and ALICE [37]. For Pb-Pb collisions at $\sqrt{s_{\rm NN}} = 2.76$ TeV CMS has also published prompt and non-prompt J/ψ production results at mid-rapidity for $p_{\rm T} > 6.5$ GeV/c [13].

In this paper we present a differential measurement of the inclusive J/ψ production at mid-rapidity in Pb-Pb collisions at $\sqrt{s_{\rm NN}} = 2.76$ TeV. The $p_{\rm T}$ dependence of the nuclear modification factor and the centrality dependence of the average transverse momentum of J/ψ have been obtained, extending the set of results presented in [12]. A measurement of the prompt and non-prompt contributions to the inclusive J/ψ production is also presented. The nuclear modification factor of non-prompt J/ψ is determined down to $p_{\rm T} = 1.5$ GeV/c and compared to model predictions.

2 Data analysis

A detailed description of the ALICE detector can be found in [38]. For the analysis presented here the detectors of the central barrel have been used, in particular the Inner Tracking System (ITS) and the Time Projection Chamber (TPC). These detectors are located inside a large solenoidal magnet with a field strength of 0.5 T. They allow the

JHEP07(2015)051

measurement of J/ψ mesons via the dielectron decay channel in the central rapidity region down to zero $p_{\rm T}$. The ITS [39] consists of six layers of silicon detectors surrounding the beam pipe at radial positions between 3.9 cm and 43.0 cm. Its two innermost layers are composed of Silicon Pixel Detectors (SPD), which provide the spatial resolution to separate on a statistical basis the non-prompt J/ψ. The active volume of the TPC [40] covers the range along the beam direction $-250 < z < 250$ cm relative to the Interaction Point (IP) and extends in radial direction from 85 cm to 247 cm. It is the main tracking device in the central barrel and is in addition used for particle identification via the measurement of the specific ionization ($\mathrm{d}E/\mathrm{d}x$) in the detector gas.

Triggering and event characterization is performed via forward detectors, the V0 [41] and two Zero Degree Calorimeters (ZDC) [42]. The V0 detectors consist of two scintillator arrays positioned at $z = -90$ cm and $z = +340$ cm and cover the pseudo-rapidity ranges $-3.7 \leq \eta \leq -1.7$ and $2.8 \leq \eta \leq 5.1$. The ZDCs, each one consisting of two quartz fiber sampling calorimeters, are placed at a distance of 114 m relative to the IP in both directions along the beam axis and are used to detect spectator nucleons.

The results presented in this article are based on data samples collected during the Pb-Pb data taking periods of the LHC in the years 2010 and 2011. In the case of the 2011 data sample the Minimum Bias (MB) Level-0 (L0) trigger condition was defined by the coincidence of signals in both V0 detectors along with a valid bunch crossing trigger. For the 2010 data sample, in addition, the detection of at least two hits in the ITS was required. Both MB trigger definitions lead to trigger efficiencies larger than 95% for inelastic Pb-Pb collisions. Electromagnetic interactions were rejected by the Level-1 (L1) trigger, which required a minimum energy deposition in the ZDC by spectator neutrons. The beam-induced background was further reduced during the offline analysis by selecting events according to the relative timing of signals in V0 and ZDC. The offline centrality selection is done using the sum of the two V0 signal amplitudes. By fitting the corresponding distribution with the results of Glauber model simulations, the average number of participants $\langle N_{\rm part}\rangle$ and the average nuclear overlap function $\langle T_{\rm AA}\rangle = \langle N_{\rm coll}\rangle/\sigma_{\rm NN}^{\rm inel}$ for a given centrality class can be determined as described in [43]. Here, $\langle N_{\rm coll}\rangle$ is the average number of binary nucleon-nucleon collisions and $\sigma_{\rm NN}^{\rm inel}$ the inelastic nucleon-nucleon cross section. The numerical values for $\langle N_{\rm part}\rangle$, $\langle N_{\rm coll}\rangle$, and $\langle T_{\rm AA}\rangle$ are tabulated in [12].

The 2010 data sample consists of 1.5×10^7 events, taken with the corresponding MB trigger. The 2011 event sample was enriched with central and semi-central Pb-Pb collisions by using thresholds on the V0 multiplicity at the L0 trigger. From the latter data set we analyzed 1.9×10^7 central (0–10% of the centrality distribution) and 1.7×10^7 semi-central (10–50%) events. The summed 2010 and 2011 data samples correspond to an integrated luminosity of $\mathcal{L}_{\rm int} = 26.4 \pm 0.3(\mathrm{stat.})^{+2.1}_{-1.7}(\mathrm{syst.})\ \mu\mathrm{b}^{-1}$ [12].

2.1 Inclusive J/ψ

J/ψ candidates are reconstructed by combining opposite-sign (OS) pairs of electron/positron candidates and calculating their invariant mass $m_{\rm ee}$. These candidates are selected from tracks reconstructed in the ITS and the TPC by employing the set of quality criteria described in [12, 44]. In order to reject the background from photon conversions in the detector material, tracks are required to have a hit in one of the SPD layers. In addition, at least 70 out of a maximum of 159 space points reconstructed in the TPC must be assigned to a given track, which also needs to fulfill a quality criterion of the track fit ($\chi^2/ndf < 4$). The tracks are required to be in the range $|\eta| < 0.8$, where the tracking and particle identification performance of the TPC is optimal, and to have $p_{\mathrm{T}} > 0.85\,\mathrm{GeV}/c$ to improve the signal-to-background ratio in the J/ψ mass region.

Electron candidates are selected by requiring that the dE/dx measurement in the TPC lies within a band $[-1\sigma, +3\sigma]$ around the momentum-dependent parameterization of the expected signal, where σ is the phase space dependent dE/dx resolution (details can be found in [45]). The selection is asymmetric in order to minimize the contribution from pions. To further suppress the hadron contamination, tracks that are compatible within $\pm 4\sigma$ with the proton expectation are rejected. A side effect of this cut is that tracks below $p_{\mathrm{T}} = 1\,\mathrm{GeV}/c$ are effectively removed.

Measurement of the inclusive J/ψ yield. The J/ψ signal counts $N_{\mathrm{J}/\psi}$ are obtained from the number of entries in the background subtracted invariant mass distributions in the range $2.92 < m_{\mathrm{ee}} < 3.16\,\mathrm{GeV}/c^2$. The uncorrelated background is evaluated with a mixed event (ME) technique. In order to achieve a good description of the background only electrons and positrons from events with similar properties in terms of centrality, primary vertex position, and event plane angle are combined. The ME distributions are scaled to the same event (SE) distributions in the mass ranges $1.5 < m_{\mathrm{ee}} < 2.5\,\mathrm{GeV}/c^2$ and $3.2 < m_{\mathrm{ee}} < 4.2\,\mathrm{GeV}/c^2$, so that the J/$\psi$ signal region is excluded. The normalization area contains the ψ(2S) signal, but its contribution is negligible and can therefore be safely ignored. Also, contributions from the tail of the J/ψ signal shape to this mass interval are below the percent level and will thus not significantly affect the normalization. Figure 1 shows a comparison of the SE and ME invariant mass distributions for the 0–40% most central Pb-Pb collisions for electron-positron pairs at mid-rapidity ($|y| < 0.8$) in two p_{T} intervals: 0–2.5 GeV/c and 2.5–6 GeV/c. The agreement between the SE and ME distributions outside the signal region is very good and allows signal extraction with significances larger than eight.

The J/ψ yield per MB event in a given p_{T} interval, $Y_{\mathrm{J}/\psi}$, is obtained as

$$Y_{\mathrm{J}/\psi}(p_{\mathrm{T}}) = \frac{N_{\mathrm{J}/\psi}(p_{\mathrm{T}})}{\mathrm{BR}_{\mathrm{ee}}\ N_{\mathrm{evts}}\ \langle A \times \epsilon \rangle (p_{\mathrm{T}})}\,. \tag{2.1}$$

Here $\mathrm{BR}_{\mathrm{ee}}$ is the branching ratio for the decay J/$\psi \to \mathrm{e}^+\mathrm{e}^-$, N_{evts} the number of events, and $\langle A \times \epsilon \rangle$ the phase space dependent product of acceptance A and reconstruction efficiency ϵ. The latter is calculated from Monte Carlo (MC) simulations as the ratio between the number of reconstructed and generated MC J/ψ, which are assumed to be unpolarized. In pp collisions at $\sqrt{s} = 7\,\mathrm{TeV}$ the J/ψ polarization has been measured and was found to be compatible with zero at mid-rapidity ($p_{\mathrm{T}} > 10\,\mathrm{GeV}/c$) and forward rapidity ($p_{\mathrm{T}} > 2\,\mathrm{GeV}/c$) [46–48]. In heavy-ion collisions no measurement exists, but J/ψ mesons produced from the recombination of charm quarks in the medium are expected to be un-

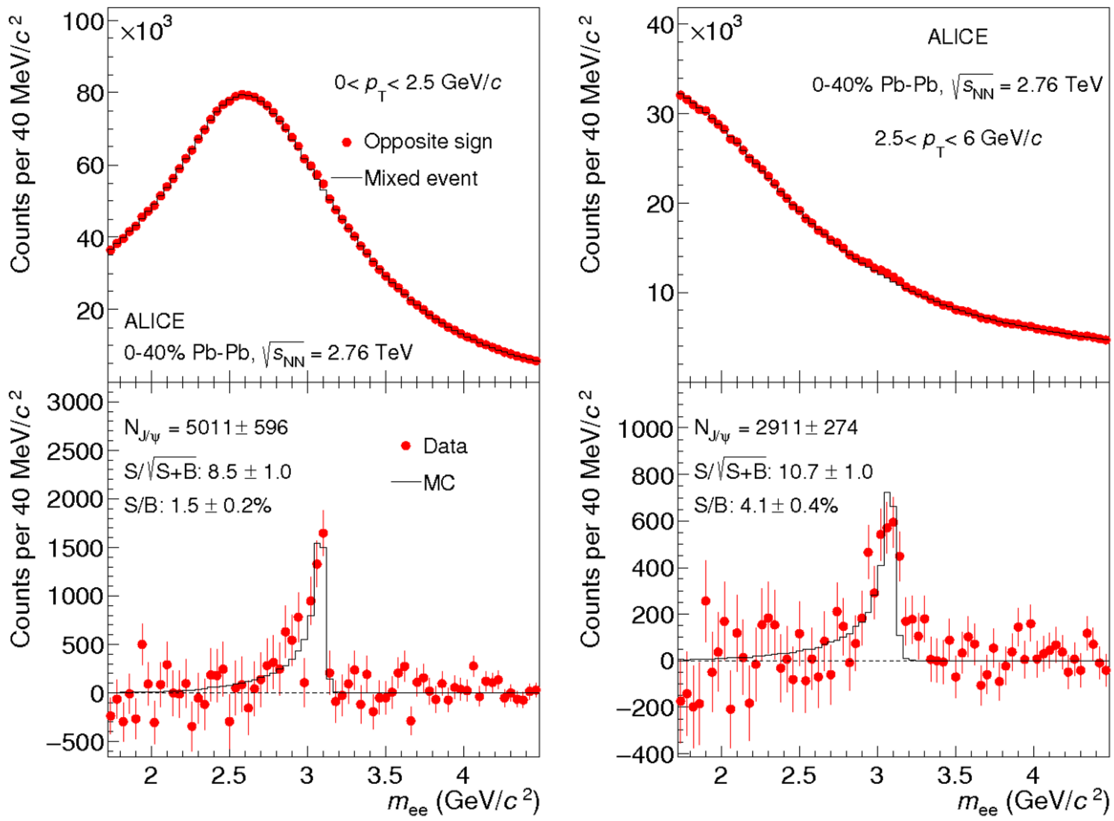

Figure 1. The invariant mass distributions of inclusive J/ψ at mid-rapidity ($|y| < 0.8$) for Pb-Pb collisions (0–40% most central) at $\sqrt{s_{NN}} = 2.76\,$TeV. The left panels show the interval $0 < p_T < 2.5\,$GeV/c and the right ones $2.5 < p_T < 6\,$GeV/c. The upper panels display the opposite sign distributions together with the result of the mixed event procedure. In the lower panels the background subtracted distributions are shown and compared to the simulated line shape. Also, the signal-to-background ratio S/B and the significance of the signal are given.

polarized.[1] The MC events used for the calculation of $\langle A \times \epsilon \rangle$ are constructed by adding to background events, generated with the HIJING model [49], J/ψ mesons decaying into e^+e^- pairs, whose phase space distribution is obtained from extrapolations of other measurements [50], taking into account shadowing effects as parameterized in EKS98 [51]. The dielectron decay is simulated with the EvtGen [52] package, using the PHOTOS model [53] to describe the influence of final state radiation. This choice, together with the simulation of bremsstrahlung in the detector material, is mandatory for a proper description of the low mass tail in the measured J/ψ mass distribution and ensures that the fraction of the signal outside of the m_{ee} integration window is properly accounted for in the correction $\langle A \times \epsilon \rangle$. The propagation of the simulated particles is done by GEANT3 [54] and a full simulation of the detector response is performed. The same reconstruction procedure and cuts are applied to MC events and to real data. The quality of the simulation is illustrated by the good agreement of the background-subtracted invariant mass distributions with the

[1]The impact of the polarization on the acceptance was studied for extreme polarization scenarios in [44].

JHEP07(2015)051

MC simulation of the J/ψ signal shape, after normalizing it to the same integral as the measured signal (see figure 1).

The analysis has been performed in two slightly different centrality intervals (0–40% and 0–50%), where the larger one is used for the extraction of non-prompt J/ψ which requires a higher statistics than the inclusive measurement. Also, the p_{T} intervals have been optimized for the different analyses. It was checked that the results for inclusive J/ψ obtained with the two centrality binnings are in good agreement.

Determination of the pp reference for R_{AA}. From the corrected J/ψ yield $Y_{\mathrm{J}/\psi}(p_{\mathrm{T}})$ the nuclear modification factor $R_{\mathrm{AA}}(p_{\mathrm{T}})$ is calculated as

$$R_{\mathrm{AA}}(p_{\mathrm{T}}) = \frac{Y_{\mathrm{J}/\psi}(p_{\mathrm{T}})}{\langle T_{\mathrm{AA}}\rangle\, \sigma^{\mathrm{pp}}_{\mathrm{J}/\psi}(p_{\mathrm{T}})}\,. \tag{2.2}$$

Since no differential J/ψ measurement at mid-rapidity at low p_{T} is available for pp collisions at $\sqrt{s} = 2.76\,\mathrm{TeV}$ [55], the reference needed for the construction of R_{AA} is based on an interpolation of the mid-rapidity measurements by PHENIX at $\sqrt{s} = 0.2\,\mathrm{TeV}$ [56], CDF at $\sqrt{s} = 1.96\,\mathrm{TeV}$ [57], and ALICE at $\sqrt{s} = 7\,\mathrm{TeV}$ [55]. The interpolated p_{T} distribution is obtained by fitting the following parameterization to the available data sets [50]

$$\frac{1}{\mathrm{d}\sigma/\mathrm{d}y}\frac{\mathrm{d}^2\sigma}{\mathrm{d}z_{\mathrm{T}}\mathrm{d}y} = c\,\frac{z_{\mathrm{T}}}{(1+a^2 z_{\mathrm{T}}^2)^n}\,. \tag{2.3}$$

Here, z_{T} is defined as $p_{\mathrm{T}}/\langle p_{\mathrm{T}}\rangle$, $a = \Gamma(3/2)\ \Gamma(n-3/2)/\Gamma(n-1)$, and $c = 2(n-1)\ a$, where n is the only free fit parameter. The value for $\langle p_{\mathrm{T}}\rangle$ (calculated in the p_{T} range 0–10 GeV/c) at $\sqrt{s} = 2.76\,\mathrm{TeV}$, which is needed to translate this parameterization into $\mathrm{d}\sigma/\mathrm{d}p_{\mathrm{T}}$, is determined by interpolating between the existing $\langle p_{\mathrm{T}}\rangle$ measurements for pp and p$\bar{\mathrm{p}}$ collisions [55–57]. This interpolation is done using various functional forms for the $\sqrt{s}$ dependence to determine the systematic uncertainty. For the absolute normalization of the parametrized spectrum, the same interpolated value $\mathrm{d}\sigma/\mathrm{d}y = 4.25 \pm 0.28(\mathrm{stat.}) \pm 0.43(\mathrm{syst.})\ \mu\mathrm{b}$ as in [12] is used.

The main sources of systematic uncertainties for the p_{T} dependent R_{AA} of inclusive J/ψ are the signal reconstruction procedure, the MC input kinematics, the uncertainties on the interpolated pp reference and on the nuclear overlap function. The corresponding values are summarized in table 1. While the first two components are uncorrelated between the p_{T} intervals (type II), the uncertainty due to the nuclear overlap function is fully correlated (type I). The pp reference on the other hand introduces both uncorrelated and correlated contributions. To determine the uncertainty related to the signal reconstruction, the normalization range of the ME background and the size and positions of the m_{ee} bins have been varied. All track and electron selection criteria, such as the electron inclusion cut and the SPD hit requirement, have been relaxed and/or tightened in order to test the stability of the result, as was performed in [12]. The value of the systematic uncertainty is determined as the standard deviation of the distribution of all results obtained with the listed variations. The evaluation of the uncertainties associated with the MC input kinematics is also described in [12], while the uncertainty of the pp reference is estimated

JHEP07(2015)051

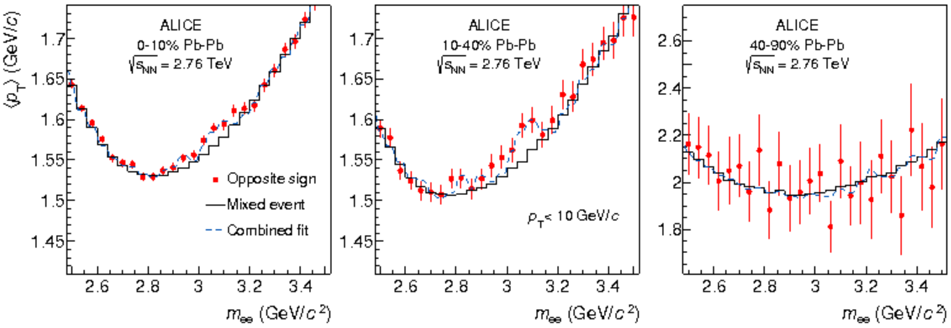

Figure 2. The average transverse momentum $\langle p_{\mathrm{T}} \rangle$ of $\mathrm{e^+e^-}$ pairs, measured for the p_{T} range 0–10 GeV/c, as a function of the invariant mass m_{ee} in centrality selected Pb-Pb collisions at $\sqrt{s_{\mathrm{NN}}} = 2.76$ TeV. The shown uncertainties are statistical only. The background $\langle p_{\mathrm{T}} \rangle$ distributions and the total fit results are also shown superimposed to the data points.

from the differences between the cross-section values obtained with the fitting procedure based on eq. (2.3) and the measured values used for the fit at the various energies.

Determination of $\langle p_{\mathrm{T}} \rangle$ and $\langle p^2_{\mathrm{T}} \rangle$. Since the collected Pb-Pb statistics would allow the extraction of the J/ψ yield in a few p_{T} intervals only, the average transverse momentum $\langle p_{\mathrm{T}} \rangle$ is determined by a fit to the distribution of the $\langle p_{\mathrm{T}} \rangle$ of $\mathrm{e^+e^-}$ pairs as a function of m_{ee}. When building such a distribution, the individual $\mathrm{e^+e^-}$ pairs are weighted by the inverse of their acceptance times efficiency $(A \times \epsilon)^{-1}$, assuming that they come from the decay of a J/ψ. The resulting $\langle p_{\mathrm{T}} \rangle$ distributions are fitted by the expression

$$\langle p_{\mathrm{T}} \rangle_{\mathrm{meas}} = \frac{1}{S(m_{\mathrm{ee}}) + B(m_{\mathrm{ee}})} \left[S(m_{\mathrm{ee}}) \, \langle p_{\mathrm{T}} \rangle_{\mathrm{J}/\psi} + B(m_{\mathrm{ee}}) \, \langle p_{\mathrm{T}} \rangle_{\mathrm{Bkg}} \right] . \tag{2.4}$$

Both factors S and B depend on m_{ee} and correspond to the distribution of the J/ψ signal and of the background. For S the same background subtracted signal distribution $S(m_{\mathrm{ee}})$ is used as for the extraction of the yield (see lower panels of figure 1), while the background B is generated from the ME sample, as $B(m_{\mathrm{ee}}) = c_{\mathrm{B}} \, B_{\mathrm{ME}}(m_{\mathrm{ee}})$. The normalization factor is determined by fitting $c_{\mathrm{B}} \, B_{\mathrm{ME}}(m_{\mathrm{ee}})$ to the corresponding m_{ee} distribution of $\mathrm{e^+e^-}$ pairs in the regions $1.5 < m_{\mathrm{ee}} < 2.5\,\mathrm{GeV}/c^2$ and $3.2 < m_{\mathrm{ee}} < 4.2\,\mathrm{GeV}/c^2$, thus excluding the signal region. For the sum $S(m_{\mathrm{ee}})+B(m_{\mathrm{ee}})$ in the denominator of eq. (2.4), the measured OS pair m_{ee} distribution is used. The $\langle p_{\mathrm{T}} \rangle_{\mathrm{Bkg}}$, defined as the $\langle p_{\mathrm{T}} \rangle$ of the combinatorial background pairs, is also calculated from the ME sample. This analysis is performed in three different centrality intervals: 0–10%, 10–40%, and 40–90%. Figure 2 shows the measured $\langle p_{\mathrm{T}} \rangle$ of the $\mathrm{e^+e^-}$ pairs in the p_{T} range 0–10 GeV/c together with the results of the fit procedure. In addition, with an equivalent method, the mean square transverse momentum $\langle p^2_{\mathrm{T}} \rangle$ is also calculated for the same centrality intervals.

The systematic uncertainties of the $\langle p_{\mathrm{T}} \rangle$ measurement for inclusive J/ψ are mainly determined by the signal extraction, the stability of track and electron selection criteria and the fit procedure (see table 2). While the first two components are not correlated between the different centrality intervals (type II), the systematic uncertainty intrinsic to the fit procedure can affect the data points in a correlated way (type I). The uncertainties

JHEP07(2015)051

Source	p_{T} range (GeV/c) 0–40% 0–2.5	2.5–6	0–50% 0–1.5	1.5–4.5	4.5–10	Type
Signal reconstruction	10.9	11.0	22.6	8.5	10.0	II
MC input kinematics	3.2	5.9	1.5	4.7	5.3	II
Nuclear overlap function $\langle T_{\mathrm{AA}} \rangle$	3.2	3.2	3.8	3.8	3.8	I
pp reference	12.1	12.1	12.1	12.1	12.1	I
	4.5	4.9	5.0	4.3	10.1	II
Total	12.6	12.6	12.7	12.7	12.7	I
	12.3	13.5	23.2	10.6	15.2	II

Table 1. The correlated (type I) and uncorrelated (type II) systematic uncertainties (in percent) on the measurement of the nuclear modification factor R_{AA} of inclusive J/ψ for several p_{T} intervals in Pb-Pb collisions (0–40% and 0–50% most central) at $\sqrt{s_{\mathrm{NN}}} = 2.76\,\mathrm{TeV}$.

Source	Centrality 0–10%	10–40%	40–90%	type
Signal extraction	2.0	1.6	4.5	II
Track selection	3.1	3.9	13.7	II
Stability of the fit procedure (from MC)	2.0	2.0	2.0	I
Total	2.0	2.0	2.0	I
	3.7	4.2	14.4	II

Table 2. The correlated (type I) and uncorrelated (type II) systematic uncertainties (in percent) on the measurement of the average transverse momentum $\langle p_{\mathrm{T}} \rangle$ of inclusive J/ψ in three centrality intervals in Pb-Pb collisions at $\sqrt{s_{\mathrm{NN}}} = 2.76\,\mathrm{TeV}$.

related to the signal extraction have been evaluated by varying the normalization range of the ME background, the size and positions of the m_{ee} bins, the fit region and by using in addition to the ME background a linear function for the background description. In addition, the stability of the fit procedure was tested by modifying the approach, e.g. by using in the fit the direct sum of S and B, instead of the OS pair m_{ee} distribution, or by using a fit function for B, instead of ME. It was also verified by applying the above described method to MC events, which were constructed by combining signal with background events with a realistic S/B ratio. It turned out that the procedure allows to recover the $\langle p_{\mathrm{T}} \rangle$ of the simulated J/ψ mesons within a 2% difference. This value is assumed as correlated (type I) uncertainty. Finally, the uncertainty in the signal-to-background ratio is propagated into the statistical uncertainty of the $\langle p_{\mathrm{T}} \rangle_{\mathrm{J}/\psi}$.

2.2 Non-prompt J/ψ

The candidate selection for the non-prompt J/ψ analysis includes, in addition to the previously described criteria, the condition that at least one of the two decay tracks has a hit in the first SPD layer, in order to enhance the resolution of secondary vertices.

The non-prompt J/ψ fraction has been determined using an unbinned two-dimensional log-likelihood fit described in detail in [37], which is performed by maximizing the quantity

$$\ln L = \sum^{N} \ln \left[f_{\rm Sig} \cdot F_{\rm Sig}(x) \cdot M_{\rm Sig}(m_{\rm ee}) + (1 - f_{\rm Sig}) \cdot F_{\rm Bkg}(x) \cdot M_{\rm Bkg}(m_{\rm ee}) \right] , \qquad (2.5)$$

where N is the total number of OS candidates in the range $2.2 < m_{\rm ee} < 4\,{\rm GeV}/c^2$ and x is the pseudo-proper decay length of the candidate

$$x = \frac{c\,(\vec{L} \cdot \vec{p_{\rm T}}/p_{\rm T})\, m_{{\rm J}/\psi}}{p_{\rm T}} . \qquad (2.6)$$

Here $\vec{L}$ is the vector pointing from the primary vertex to the J/ψ decay vertex and $m_{{\rm J}/\psi}$ the mass of the J/ψ taken from [58]. $F_{\rm Sig}(x)$ and $F_{\rm Bkg}(x)$ ($M_{\rm Sig}(m_{\rm ee})$ and $M_{\rm Bkg}(m_{\rm ee})$) are Probability Density Functions (p.d.f.) describing the pseudo-proper decay length (invariant mass) distribution for signal and background candidates, respectively. $F_{\rm Sig}(x)$ is defined as

$$F_{\rm Sig}(x) = f'_{\rm B} \cdot F_{\rm B}(x) + (1 - f'_{\rm B}) \cdot F_{\rm prompt}(x) , \qquad (2.7)$$

where $F_{\rm prompt}(x)$ and $F_{\rm B}(x)$ are the p.d.f. for prompt and non-prompt J/ψ, respectively, and $f'_{\rm B}$ is the fraction of *reconstructed* J/ψ coming from beauty hadron decays

$$f'_{\rm B} = \frac{N_{{\rm J}/\psi \leftarrow h_B}}{N_{{\rm J}/\psi \leftarrow h_B} + N_{\rm prompt}} . \qquad (2.8)$$

A correction due to different average $\langle A \times \epsilon \rangle$ values, in a given $p_{\rm T}$ interval, for prompt and non-prompt J/ψ, is necessary to obtain from $f'_{\rm B}$ the fraction of *produced* non-prompt J/ψ, $f_{\rm B}$

$$f_{\rm B} = \left(1 + \frac{1 - f'_{\rm B}}{f'_{\rm B}} \frac{\langle A \times \epsilon \rangle_{\rm B}}{\langle A \times \epsilon \rangle_{\rm prompt}} \right)^{-1} . \qquad (2.9)$$

The various ingredients for the determination of $f_{\rm B}$ are described in the following:

Monte Carlo $p_{\rm T}$ distributions and polarization assumptions. Assuming both prompt and non-prompt J/ψ to be unpolarized, at a given $p_{\rm T}$ their acceptance times efficiency values $\langle A \times \epsilon \rangle$ are the same. However, the $p_{\rm T}$ distributions of prompt and non-prompt J/ψ can be different, resulting in different average $\langle A \times \epsilon \rangle$ computed over a $p_{\rm T}$ range of finite size. Different hypotheses for the kinematical ($p_{\rm T}$) distributions of both prompt and non-prompt J/ψ are considered, i.e. including or excluding shadowing or suppression effects as, e.g., those predicted in references [59–61] for non-prompt J/ψ. Due to the weak $p_{\rm T}$ dependence of $\langle A \times \epsilon \rangle$, the resulting uncertainty on $f_{\rm B}$ is small, being $\sim 5\%$ at low $p_{\rm T}$ and $\sim 3\%$ in the highest $p_{\rm T}$ bin, and is independent of centrality.

At a given $p_{\rm T}$, prompt and non-prompt J/ψ can have different polarization and therefore a different acceptance. However, the polarization of J/ψ from b-hadron decays is expected to be small due to the averaging effect caused by the admixture of various exclusive B $\rightarrow$ J/ψ+X decay channels. Indeed, in more elementary colliding systems, the sizable polarization, which is observed when the polarization axis refers to the B-meson direction [62], is strongly smeared when calculated with respect to the direction of the daughter J/ψ [63], as observed by CDF [64]. The central values of the fraction of non-prompt J/ψ are evaluated with eq. (2.9) assuming unpolarized prompt J/ψ and a polarization of non-prompt J/ψ as predicted by EVTGEN [52]. The assumption of a null polarization for non-prompt J/ψ results in a relative decrease of $f_{\rm B}$ by only 1% at high $p_{\rm T}$ (4.5–10 GeV/c) and 3% at low $p_{\rm T}$ (1.5–4.5 GeV/c). The relative variations of $f_{\rm B}$ expected in extreme scenarios for the polarization of prompt J/ψ was studied in [44]. The uncertainties related to the polarization of prompt and non-prompt J/ψ are are not further propagated to the results.

P.d.f. for prompt J/ψ: $F_{\rm prompt}(x)$. The x distribution $F_{\rm prompt}(x)$ for prompt J/ψ, which decay at the primary vertex, coincides with the resolution function $R(x)$, which describes the accuracy by which x can be reconstructed. It also enters in the p.d.f. describing the x distributions of non-prompt J/ψ, $F_{\rm B}(x)$, and of the background candidates, $F_{\rm Bkg}(x)$. The determination of $R(x)$ is based on the same MC data sample as used for the inclusive J/ψ analysis (see section 2.1). The systematic uncertainty on $R(x)$ was estimated with a MC approach by propagating the maximum observed discrepancies of the track parameters (space and momentum variables) between data and MC to the x variable [45, 65, 66] and was found to be at most 10%. To propagate this systematic uncertainty to the final results the fits are repeated after modifying in the log-likelihood function the resolution to $(1/(1+\delta)) \times R\,(x/(1+\delta))$. In this expression δ parameterizes the relative variation of the RMS of the resolution function and is varied between -10% and $+10\%$. The systematic uncertainty due to the resolution function is smaller in the highest $p_{\rm T}$ bin, because of the better resolution in the x variable and the higher values of the signal-to-background ratio.

P.d.f. for non-prompt J/ψ: $F_{\rm B}(x)$. The shape of the x distribution of non-prompt J/ψ is estimated by using PYTHIA 6.4.21 [67] in the Perugia-0 tune [68] to generate beauty hadrons at $\sqrt{s} = 2.76$ TeV, and the EvtGen package [52] to describe their decays. The systematic uncertainty related to this shape is estimated by assuming a softer $p_{\rm T}$ distribution for the non-prompt J/ψ which is obtained by adding the suppression effects as predicted in [61] and a harder one taken from the same PYTHIA event generator at $\sqrt{s} = 7$ TeV instead of 2.76 TeV. The resulting systematic uncertainty is within 3–4%.

P.d.f. for the background: $F_{\rm Bkg}(x)$. The main difference of the analysis presented in this section, with respect to previous work on pp collisions [37], concerns the description of $F_{\rm Bkg}(x)$. In this analysis such a function includes an extra symmetric exponential tail ($\propto e^{-|x|/\lambda_{\rm sym}}$) [57] and depends on the invariant mass and the $p_{\rm T}$ of the dielectron pair. It is determined, for each centrality class, by a fit to the data in three $p_{\rm T}$ regions (1.5–3, 3–4.5, 4.5–10 GeV/c) and in four invariant mass regions on the side-bands of the J/ψ mass peak (2.2–2.6, 2.6–2.8, 3.16–3.5, 3.5–4 GeV/c^2, labelled with the indices 1, 2, 3 and 4, respectively), for a total of 3×4 combinations. The background function in the invariant mass region 2.8–3.16 GeV/c^2 and in each of the three $p_{\rm T}$ ranges are obtained by an interpolation procedure as the weighted combination of the p.d.f. determined in the other four invariant mass regions. The weights are chosen inversely proportional to the absolute difference (or its square) between the mean of the invariant mass distribution in the given mass interval and that in the interpolated region

$$F_{\mathrm{Bkg}_{\mathrm{interp}}}(x) = \sum_{i=1}^{4} w_i \, F_{\mathrm{Bkg}_i}(x); \quad w_i \propto |\langle m_{\mathrm{ee}}\rangle_i - \langle m_{\mathrm{ee}}\rangle_{\mathrm{interp}}|^{-n} \qquad (n \;=\; 1 \text{ or } 2). \tag{2.10}$$

Optionally, only the two adjacent mass regions can be considered in the interpolation procedure, corresponding to the condition $w_1 = w_4 = 0$. The central value of f_{B} has been determined as the average of the values obtained with the different assumptions ($n = 1$ or $n = 2$, with or without the condition $w_1 = w_4 = 0$). The RMS of the distributions of the relative variations obtained for f_{B} is used to define the systematic uncertainty. It becomes larger for central events and in the lowest p_{T} interval, where the signal-to-background ratio S/B is lower. This approach allows to cope with the much lower S/B ratio in Pb-Pb than in pp collisions.

P.d.f. for the invariant mass distribution of the signal: $M_{\mathrm{Sig}}(m_{\mathrm{ee}})$. The shape of the invariant mass distribution for the signal is determined by the same MC simulations described in section 2.1. The influence of detector material budget is studied with dedicated MC simulations, where the material budget is varied within its uncertainty (±6%) [69]. The resulting contribution to the systematic uncertainty on f_{B} slightly increases for central events, and ranges from 2 to 4%.

P.d.f. for the invariant mass distribution of the background: $M_{\mathrm{Bkg}}(m_{\mathrm{ee}})$. The shape of the invariant mass distribution for the background candidates is determined from ME pairs. The related systematic uncertainty on f_{B} is evaluated using the like-sign distribution, instead of the ME one. The uncertainty increases at higher centrality and in the lowest p_{T} interval due to the decrease of the S/B ratio.

As an example in figure 3 the projections of the best fit function for $n = 1$ and $w_1 = w_4 = 0$ are shown superimposed to the invariant mass (upper panel) and x (lower panel) distributions of the candidates in the centrality range 10–50% for $1.5 < p_{\mathrm{T}} < 10\,\mathrm{GeV}/c$.

A summary of the systematic uncertainties on the determination of the non-prompt J/ψ fraction is provided in table 3 for the three centrality intervals in the integrated p_{T} range and, in the two p_{T} ranges where the results will be given, for the most central collisions (0–10%).

The value of f_{B} is determined in two p_{T} bins (1.5–4.5 and 4.5–10 GeV/c) for the 0–50% centrality range and in three centrality classes (0–10%, 10–40% and 40–90%) for $1.5 < p_{\mathrm{T}} < 10\,\mathrm{GeV}/c$. The f_{B} measurements are then combined with the nuclear modification factors of inclusive J/ψ to get the non-prompt and prompt J/ψ R_{AA}

$$R_{\mathrm{AA}}^{\text{non-prompt J}/\psi} = \frac{f_{\mathrm{B}}^{\mathrm{Pb-Pb}}}{f_{\mathrm{B}}^{\mathrm{pp}}} R_{\mathrm{AA}}^{\text{incl. J}/\psi}\,, \qquad R_{\mathrm{AA}}^{\text{prompt J}/\psi} = \frac{1 - f_{\mathrm{B}}^{\mathrm{Pb-Pb}}}{1 - f_{\mathrm{B}}^{\mathrm{pp}}} R_{\mathrm{AA}}^{\text{incl. J}/\psi}\,. \tag{2.11}$$

pp interpolation. The value of f_{B} in pp collision at $\sqrt{s} = 2.76\,\mathrm{TeV}$, $f_{\mathrm{B}}^{\mathrm{pp}}$, is needed to compute the R_{AA} for prompt and non-prompt J/ψ mesons, see eq. (2.11). It is determined by an interpolation procedure. Therefore, a fit is performed to the existing measurements of

JHEP07(2015)051

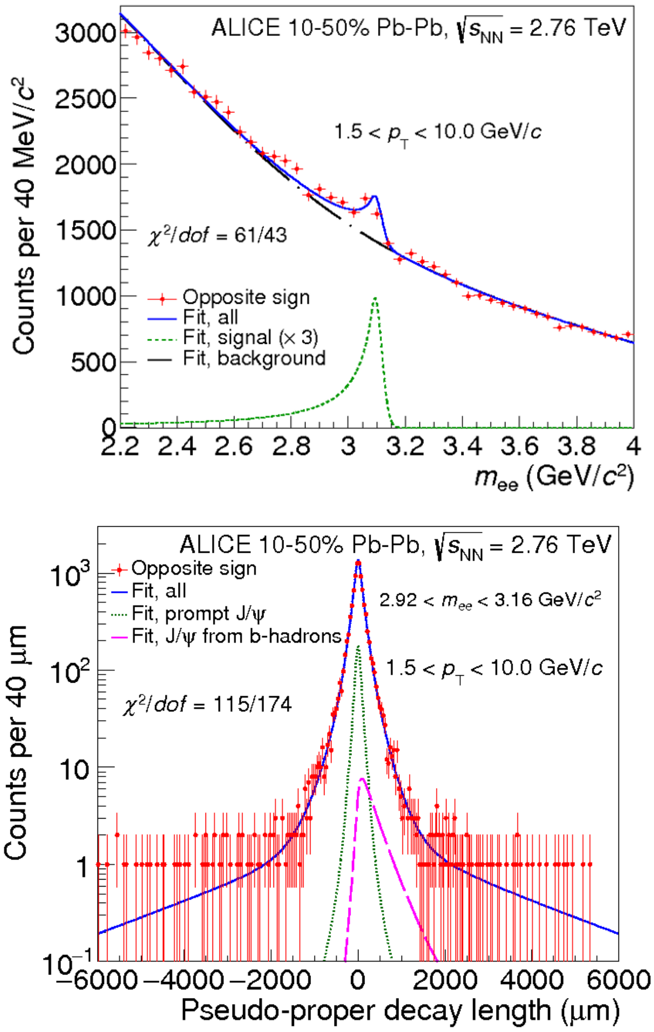

Figure 3. The invariant mass (upper panel) and pseudo-proper decay length (lower panel) distributions for $\mathrm{e}^+\mathrm{e}^-$ pairs with $p_{\mathrm{T}} > 1.5\,\mathrm{GeV}/c$ in Pb-Pb collisions in the centrality interval 10–50% at $\sqrt{s_{\mathrm{NN}}} = 2.76\,\mathrm{TeV}$. The projections of the maximum likelihood fit used to extract f_{B} are superimposed to the data.

f_{B} as a function of p_{T} in mid-rapidity pp collisions at $\sqrt{s} = 7\,\mathrm{TeV}$ (ALICE [37], ATLAS [35] and CMS [70]). The function used to fit the data is chosen as

$$f_{\mathrm{B}}^{\mathrm{model}}(p_{\mathrm{T}}) = \frac{d\sigma^{\mathrm{FONLL}}_{\mathrm{J}/\psi\leftarrow h_{\mathrm{B}}}}{dp_{\mathrm{T}}} \Bigg/ \frac{d\sigma^{\mathrm{phenom.}}_{\mathrm{J}/\psi}}{dp_{\mathrm{T}}}\,, \tag{2.12}$$

which is the ratio of the differential cross section for non-prompt J/ψ obtained by an implementation of pQCD calculations at fixed order with next-to leading-log resummation (FONLL) [71] to that for inclusive J/ψ, parameterized by the phenomenological function defined in eq. (2.3). A similar fit is then performed to the CDF results [57] in $\mathrm{p\bar{p}}$ collisions at $\sqrt{s} = 1.96\,\mathrm{TeV}$. Finally, the $f_{\mathrm{B}}^{\mathrm{pp}}(p_{\mathrm{T}})$ value at $\sqrt{s} = 2.76\,\mathrm{TeV}$ is determined by an energy interpolation, which gives $f_{\mathrm{B}}^{\mathrm{pp}} = 0.122 \pm 0.010$ in the integrated p_{T} range 1.5–

Source	$1.5 < p_{\rm T} < 10\,{\rm GeV}/c$ Centr. 0–10%	Centr. 10–40%	Centr. 40–90%	Centr. 0–10% $p_{\rm T}$ 1.5–4.5 GeV/c	$p_{\rm T}$ 4.5–10 GeV/c	Type
Resolution function	23	15	10	28	12	I
P.d.f. for non-prompt J/ψ	4	3	3	4	3	I
P.d.f. for the background	22	15	5	23	19	II
MC $p_{\rm T}$ distribution	5	5	5	5	3	I
P.d.f. for the invariant mass of signal	5	3	2	5	3	I
P.d.f. for the invariant mass of background	7	5	3	7	5	II
Total	34	23	13	38	24	

Table 3. Systematic uncertainties (in percent) on the measurement of the fraction $f_{\rm B}$ of J/ψ from the decay of beauty hadrons, for different centrality intervals in the transverse momentum range $1.5 < p_{\rm T} < 10\,{\rm GeV}/c$, and in the two $p_{\rm T}$ intervals for the most central collisions. The contributions which are fully correlated between the different centrality classes are denoted as type I, the uncorrelated ones as type II.

10 GeV/c. The quoted uncertainty includes: *(i)* a component from the fit procedure, which depends on the uncertainties of both data and FONLL predictions; *(ii)* the systematic uncertainty due to the energy interpolation, which has been estimated by considering different functional forms of the $\sqrt{s}$ dependency (linear, exponential and power law); *(iii)* an additional systematic uncertainty, which has been obtained by repeating the whole fitting procedure after excluding, one at a time, the data samples used for the $f_{\rm B}$ fit in pp collisions at $\sqrt{s} = 7\,{\rm TeV}$.

3 Results

Figure 4 shows the $\langle p_{\rm T}\rangle$ of inclusive J/ψ for the three analyzed centrality intervals. The numerical values for $\langle p_{\rm T}\rangle$ are summarized in table 4. As a reference, the $\langle p_{\rm T}\rangle$ in pp collisions at the same centre-of-mass energy, as determined by the interpolation method described in section 2.1, is also presented. The $\langle p_{\rm T}\rangle$ for Pb-Pb collisions is significantly smaller than that for pp collisions. Such a behaviour is not observed at smaller centre-of-mass energies (see left panel of figure 4), for which no significant system size dependence of $\langle p_{\rm T}\rangle$ is seen. This might indicate the onset of processes which either deplete the high $p_{\rm T}$ region or enhance the J/ψ production at low $p_{\rm T}$ in heavy-ion collisions at the LHC. The latter effect would be expected as a consequence of a significant contribution from c$\bar{\rm c}$ coalescence.

It has been suggested [77] that the observable $r_{\rm AA} = \langle p_{\rm T}^2\rangle_{\rm AA}/\langle p_{\rm T}^2\rangle_{\rm pp}$ should be particularly sensitive to medium modifications affecting the J/ψ transverse momentum distributions. The measured $\langle p_{\rm T}^2\rangle$ values for Pb-Pb collisions at $\sqrt{s_{\rm NN}} = 2.76\,{\rm TeV}$ are summarized in table 4. The corresponding $r_{\rm AA}$ values as a function of $\langle N_{\rm part}\rangle$ are shown in figure 5 and are found to be significantly below unity. This is in contrast to results from lower centre-of-mass energies, where either values consistent with unity (PHENIX at $\sqrt{s_{\rm NN}} = 0.2\,{\rm TeV}$ [9, 72]) or around 1.5 (NA50 at $\sqrt{s_{\rm NN}} = 17.3\,{\rm GeV}$ [73]) were obtained (see left panel of figure 5). The measured $\langle N_{\rm part}\rangle$ dependences of $\langle p_{\rm T}\rangle$ and $r_{\rm AA}$ are compared with a transport model for inclusive J/ψ by Zhao et al. [75, 76] in the right panels of figures 4 and 5. This model includes regeneration and dissociation processes, based on in-medium

JHEP07(2015)051

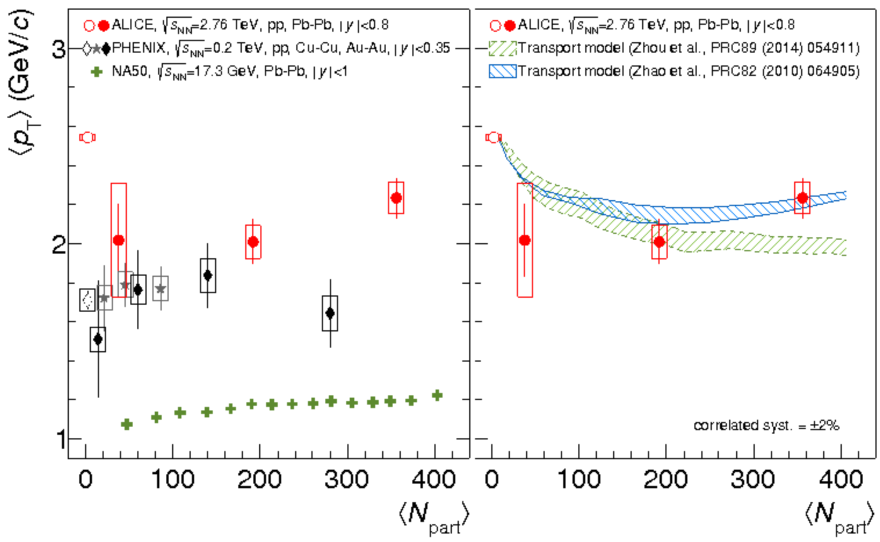

Figure 4. The average transverse momentum $\langle p_T \rangle$ of inclusive J/ψ measured at mid-rapidity ($|y| < 0.8$) in centrality selected Pb-Pb collisions (filled circles) and pp collisions (open circles) at $\sqrt{s_{NN}} = 2.76$ TeV as a function of the number of participants $\langle N_{part} \rangle$. The uncorrelated systematic uncertainties (type II) are depicted by the open boxes. Left panel: a comparison to results obtained by the PHENIX collaboration for Au-Au and Cu-Cu collisions at $\sqrt{s_{NN}} = 0.2$ TeV [9, 72] (open and filled diamonds) and by the NA50 collaboration for Pb-Pb collisions at $\sqrt{s_{NN}} = 17.3$ GeV [73] (crosses). The $\langle p_T \rangle$ values are calculated for NA50 and PHENIX in the p_T interval 0–5 GeV/c, while for ALICE the p_T interval is 0–10 GeV/c. Right panel: $\langle p_T \rangle$ is compared to theory predictions by Zhou et al. [74] and Zhao et al. [75, 76] for the p_T interval 0–10 GeV/c.

Centrality	$\langle p_T \rangle$ (GeV/c)	$\langle p_T^2 \rangle$ (GeV$^2/c^2$)
0–10%	$2.23 \pm 0.10 \pm 0.08$	$5.50 \pm 0.58 \pm 0.25$
10–40%	$2.01 \pm 0.12 \pm 0.08$	$4.97 \pm 0.65 \pm 0.34$
40–90%	$2.02 \pm 0.19 \pm 0.29$	$5.15 \pm 1.05 \pm 1.23$
pp	$2.54 \pm 0.02 \pm 0.01$	$9.07 \pm 0.15 \pm 0.07$

Table 4. The numerical values of $\langle p_T \rangle$ and $\langle p_T^2 \rangle$ calculated in the range $0 < p_T < 10$ GeV/c for the three analyzed centrality intervals in Pb-Pb collisions (the first uncertainty is the statistical and the second is the uncorrelated systematic (type II), the correlated uncertainty has a value of 2%, see table 2). The values for pp collisions obtained by the interpolation procedure are given as a reference.

J/ψ spectral functions, throughout the evolution of a thermally expanding fireball. It also incorporates nuclear shadowing by reducing the input charm cross section by a factor of up to 1/3, with a centrality dependence as estimated in [78]. There is a fair agreement between our $\langle p_T \rangle$ results and the model calculation, while the r_{AA} is not described by this prediction. Our $\langle p_T \rangle$ and r_{AA} results are also compared with the calculations by Zhou et al. [74]. These calculations are also based on a transport approach and incorporate dissociation and regeneration of J/ψ and heavier charmonia, as well as nuclear shadowing

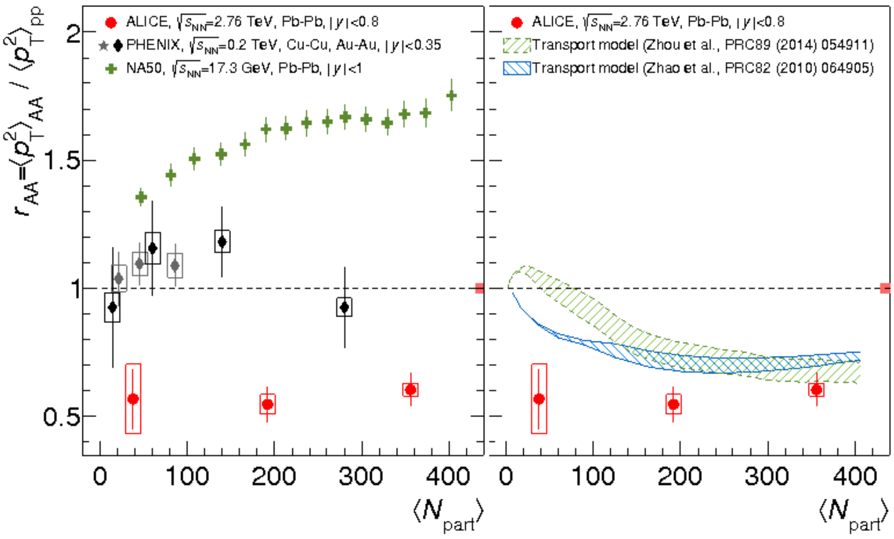

Figure 5. The ratio $r_{\rm AA} = \langle p_{\rm T}^2\rangle_{\rm AA}/\langle p_{\rm T}^2\rangle_{\rm pp}$ in the $p_{\rm T}$ interval 0–10 GeV/c for inclusive J/ψ measured at mid-rapidity ($|y| < 0.8$) in centrality selected Pb-Pb collisions (filled circles) at $\sqrt{s_{\rm NN}} = 2.76$ TeV as a function of the number of participants $\langle N_{\rm part}\rangle$. The uncorrelated systematic uncertainties (type II) are depicted by the open boxes, while correlated uncertainty (type I) is shown as the filled box at unity. Left panel: a comparison to results obtained by the PHENIX collaboration for Au-Au and Cu-Cu collisions at $\sqrt{s_{\rm NN}} = 0.2$ TeV [9, 72] (filled diamonds) and by the NA50 collaboration for Pb-Pb collisions at $\sqrt{s_{\rm NN}} = 17.3$ GeV [73] (crosses). The PHENIX and NA50 $r_{\rm AA}$ values are calculated in the $p_{\rm T}$ interval 0–5 GeV/c. Right panel: $r_{\rm AA}$ is compared to theory predictions by Zhou et al. [74] and Zhao et al. [75, 76] for the $p_{\rm T}$ interval 0–10 GeV/c.

according to EKS98 [51]. While the most central data point is matched by the prediction, it does not describe the evolution of $r_{\rm AA}$ towards peripheral collisions. It must be noted that our results from Pb-Pb collisions at forward rapidity [79] exhibit a continuous decrease of $\langle p_{\rm T}\rangle$ and $r_{\rm AA}$ from peripheral towards central events and are thus closer to the theory predictions, while the behaviour of mid-rapidity Pb-Pb results is more compatible with a flat $\langle N_{\rm part}\rangle$ dependence.

The $R_{\rm AA}$ of inclusive J/ψ in three $p_{\rm T}$ intervals is shown in figure 6 along with the results by the CMS collaboration for the interval $6.5 < p_{\rm T} < 30$ GeV/c [13], both in 0–40% most central Pb-Pb collisions. The corresponding numerical values are $0.82 \pm 0.11(\text{stat.}) \pm 0.10(\text{syst.})$ for the interval $0 < p_{\rm T} < 2.5$ GeV/c and $0.58 \pm 0.06(\text{stat.}) \pm 0.08(\text{syst.})$ for $2.5 < p_{\rm T} < 6$ GeV/c, where the systematic uncertainties quoted here are the uncorrelated (type II) ones, as listed in table 1. The data point for $4.5 < p_{\rm T} < 10$ GeV/c corresponds to the $R_{\rm AA}$ value given in table 5 (centrality range 0–50%). Table 5 also contains the $R_{\rm AA}$ values for prompt J/ψ, which are numerically identical to the ones for inclusive J/ψ. The inclusive $R_{\rm AA}$ values below $p_{\rm T} = 6$ GeV/c are significantly higher than those measured at higher $p_{\rm T}$, corresponding to a decrease of $R_{\rm AA}$ with increasing $p_{\rm T}$, while the high $p_{\rm T}$ data point is close to the CMS measurement. This $p_{\rm T}$ dependence is similar to the one observed at forward rapidity [12], and is in clear contrast to the $p_{\rm T}$ dependence measured at lower

JHEP07(2015)051

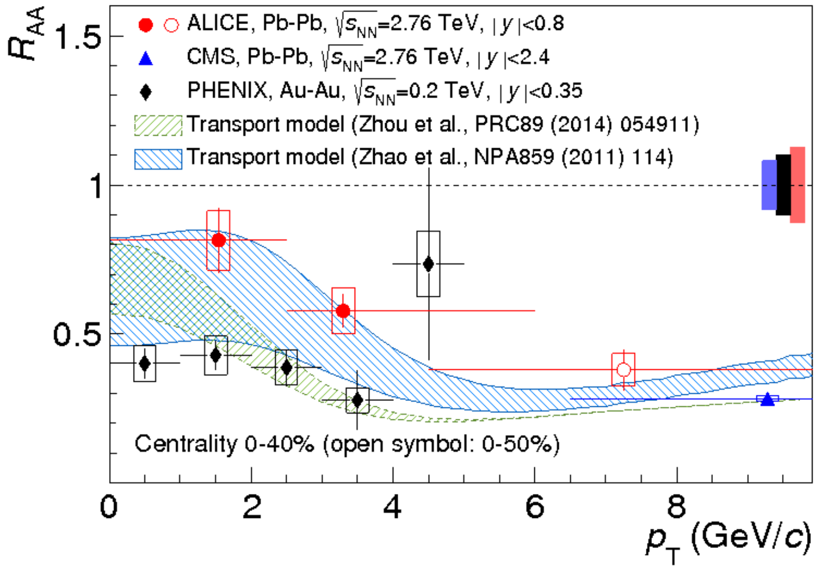

Figure 6. The nuclear modification factor R_{AA} of inclusive J/ψ, measured at mid-rapidity ($|y| < 0.8$) in Pb-Pb collisions (0–40% most central) at $\sqrt{s_{NN}} = 2.76$ TeV, as a function of transverse momentum p_T. The filled symbols are placed at the measured p_T for the given interval. Since for the data point in $4.5 < p_T < 10$ GeV/c (open symbol, 0–50% most central) $\langle p_T \rangle$ is not available due to the limited statistics, it is plotted at the centre of the p_T interval. The uncorrelated systematic uncertainties (type II) are depicted by the open boxes, while the correlated uncertainties (type I) are shown as the filled boxes at unity. The data are compared to corresponding results by PHENIX for Au-Au collisions (0–40% most central) at $\sqrt{s_{NN}} = 0.2$ TeV [9], by CMS for Pb-Pb collisions (0–40% most central) at $\sqrt{s_{NN}} = 2.76$ TeV [13], and to predictions by the model of Zhou et al. [74] and Zhao et al. [75, 76].

centre-of-mass energies by the PHENIX collaboration for $\sqrt{s_{NN}} = 0.2$ TeV [9]. Figure 6 also shows the model predictions by Zhou et al. [74]. The value of the predicted R_{AA} is systematically below the measurement and exhibits a p_T dependence similar to the one in the data. The prediction by Zhao et al. [75, 76] is close to our result. In both models, the rise of R_{AA} towards $p_T = 0$ is due to the dominant contribution from J/ψ regeneration via coalescence.

The fraction of non-prompt J/ψ in the p_T range 1.5–10 GeV/c is shown as a function of the number of participants for the centrality intervals 40–90% ($\langle N_{part} \rangle = 38$), 10–40% ($\langle N_{part} \rangle = 192$), and 0–10% ($\langle N_{part} \rangle = 356$) in the left panel of figure 7. Within uncertainties, no centrality dependence is observed. The p_T dependence of f_B (centrality: 0–50%) is shown in the right panel of figure 7 and compared with the measurements by CMS in the centrality interval 0–100% and $p_T > 6.5$ GeV/c (for the numerical values see table 5). Our results at low transverse momenta extend the CMS measurements in Pb-Pb collisions towards lower p_T. Also shown are results at mid-rapidity in pp at $\sqrt{s} = 7$ TeV (ALICE [37], ATLAS [35] and CMS [70]) and in p$\bar{\text{p}}$ collisions at $\sqrt{s} = 1.96$ TeV (CDF [57]). Considering the ALICE and CMS results in Pb-Pb collisions together, a similar p_T dependence as in pp

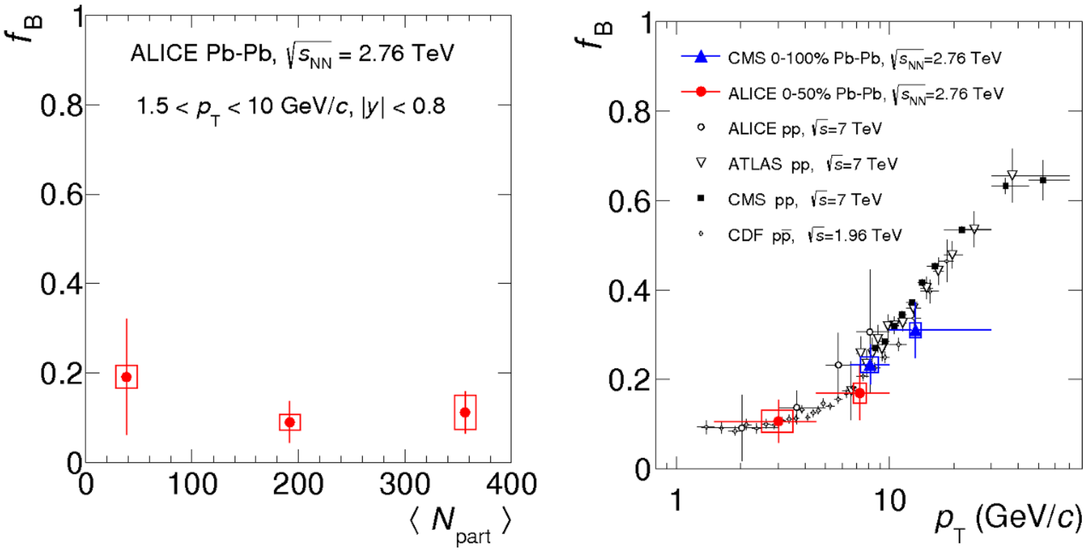

Figure 7. The fraction of J/ψ from beauty hadron decays f_{B} at mid-rapidity measured in the p_{T} interval $1.5 < p_{\mathrm{T}} < 10\,\mathrm{GeV}/c$ for centrality selected Pb-Pb collisions at $\sqrt{s_{\mathrm{NN}}} = 2.76\,\mathrm{TeV}$ (left). The p_{T} dependence of f_{B} at mid-rapidity for Pb-Pb ($\sqrt{s_{\mathrm{NN}}} = 2.76\,\mathrm{TeV}$, $|y_{\mathrm{J}/\psi}| < 0.8$) and pp ($\sqrt{s} = 7\,\mathrm{TeV}$, $|y_{\mathrm{J}/\psi}| < 0.9$) [37] collisions is compared with measurements by CDF ($|y_{\mathrm{J}/\psi}| < 0.6$) [57], ATLAS ($|y_{\mathrm{J}/\psi}| < 0.75$) [35], and CMS ($|y_{\mathrm{J}/\psi}| < 0.9$) [13, 70] (right).

p_{T}(GeV/c)	f_{B}(%)	R_{AA}(inclusive J/ψ)	R_{AA}(prompt J/ψ)	R_{AA}(non-prompt J/ψ)
0.0–1.5	–	0.89±0.20±0.21	–	–
1.5–4.5	10.7±4.8±2.5	0.76±0.09±0.08	0.76±0.10±0.08	0.73±0.34±0.20
4.5–10.0	17.0±6.1±2.2	0.38±0.07±0.06	0.38±0.07±0.06	0.37±0.15±0.09

Table 5. The numerical values on the fraction of J/ψ from beauty hadron decays f_{B} at mid-rapidity and the nuclear modification factors R_{AA} of inclusive, prompt and non-prompt J/ψ for Pb-Pb collisions at $\sqrt{s} = 2.76\,\mathrm{TeV}$. These results correspond to the centrality interval 0–50%. The first uncertainty is statistical and the second uncorrelated systematic (type II).

is observed. However, this similarity could be coincidental, being due to a compensation of the medium effects on the prompt component (J/ψ dissociation and recombination) and on the non-prompt part (b-quark energy loss).

In figure 8 the nuclear modification factor for non-prompt J/ψ for $1.5 < p_{\mathrm{T}} < 4.5\,\mathrm{GeV}/c$ and $4.5 < p_{\mathrm{T}} < 10\,\mathrm{GeV}/c$ is shown together with the result by CMS for $6.5 < p_{\mathrm{T}} < 30\,\mathrm{GeV}/c$ [13] and with theoretical model predictions [30, 31, 59–61, 80–85]. One should note that the centrality ranges are not the same for ALICE (0–50%) and CMS (0–20% and 20–100%). However, the results obtained by CMS for these two centrality bins are compatible with each other, and also compatible with our measurement in the high p_{T} interval ($4.5 < p_{\mathrm{T}} < 10\,\mathrm{GeV}/c$). The model by Uphoff et al. [61] follows a partonic transport approach based on the Boltzmann equation, which allows interactions among all partons. It does not include radiative processes for heavy quarks. The calculation has been

JHEP07(2015)051

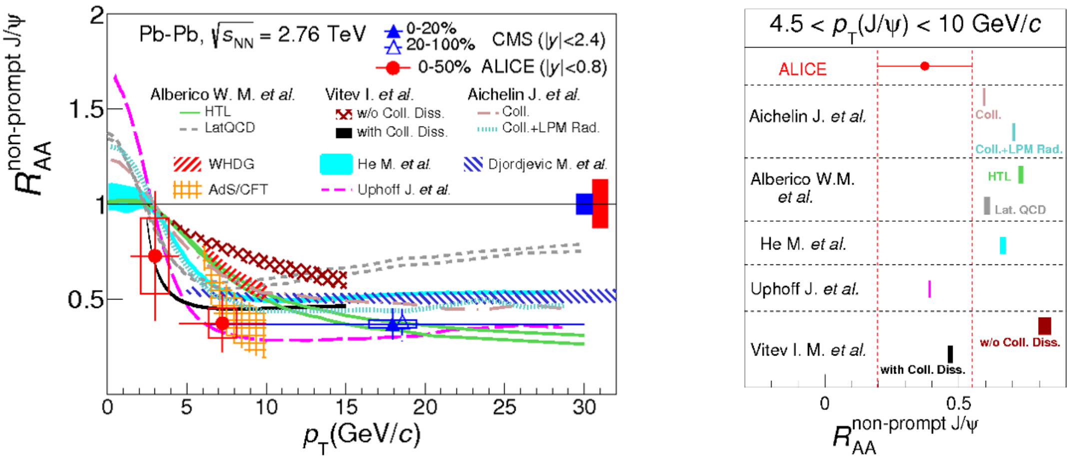

Figure 8. The nuclear modification factor $R_{\rm AA}$ at mid-rapidity ($|y| < 0.8$) for non-prompt J/ψ in Pb-Pb collisions at $\sqrt{s_{\rm NN}} = 2.76$ TeV as a function of transverse momentum $p_{\rm T}$. The ALICE measurement corresponds to the 0–50% centrality range and to the $p_{\rm T}$ intervals $1.5 < p_{\rm T} < 4.5\,{\rm GeV}/c$ and $4.5 < p_{\rm T} < 10\,{\rm GeV}/c$. The uncorrelated systematic uncertainties (type II) are depicted by the open boxes, while the correlated uncertainties (type I) are shown as filled boxes at unity. Results by CMS for higher $p_{\rm T}$ in the centrality range 0–20% and 20–100% [13] are also shown (the two points have been slightly displaced horizontally for better visibility). The data are compared to theoretical predictions at mid-rapidity (see text for details). In the right panel, the ALICE result in the $p_{\rm T}$ interval $4.5 < p_{\rm T} < 10\,{\rm GeV}/c$ is compared to theoretical predictions integrated over the same $p_{\rm T}$ range.

performed for a fixed impact parameter $b = 5$ fm. In the model of Alberico et al. [59, 60] the propagation of the heavy quarks in the medium is described by the relativistic Langevin equation. The predicted $p_{\rm T}$ dependence of $R_{\rm AA}$ is strongly influenced by the choice of transport coefficients. Two values are considered, either as provided by a perturbative calculation (hard thermal loop approach) or extracted from lattice-QCD simulations. The calculations have been provided for the centrality range 0–50%. A transport approach, which is based on a strong-coupling scheme, is employed in the model of He et al. [80]. The transport is implemented using non-perturbative interactions for heavy quarks and mesons through the QGP, hadronization and hadronic phases of a nuclear collision. In particular, the elastic heavy-quark scattering in the QGP is evaluated within a thermodynamic T-matrix approach, by generating resonances close to the critical temperature that can in turn recombine into B mesons, followed by hadronic diffusion using effective hadronic scattering amplitudes. The hydrodynamic evolution of the system is quantitatively constrained by the measured transverse momentum distributions and elliptic flow of light hadrons. Radiative processes, which should improve the description at high $p_{\rm T}$, are not included in this approach. The calculations have been performed in the centrality range 0–50%. The model of Vitev et al. [30, 31] assumes the existence of open heavy flavour bound-state solutions in the QGP in the vicinity of the critical temperature. A description of beauty quark quenching is combined with B meson inelastic breakup processes. Furthermore, modified beauty parton distribution functions and beauty fragmentation functions in a co-moving plasma are implemented in this calculation. The prediction is shown for a fixed centrality, corresponding to $\langle N_{\rm part}\rangle = 200$, a value very close to the average number of participants in the centrality range 0–50%. In the model, a sizable fraction of the suppression is ascribed to the inelastic break-up processes (collisional dissociation), as can be deduced from figure 8 by comparing the full model prediction with and without the contribution of this specific process. The model of Djordjevic [81], shown in figure 8 for the centrality range 0–50%, uses a formalism that takes into account finite size dynamical QCD medium with finite magnetic mass effects and running coupling. In the WHDG model [82] (centrality range 0–50%) the energy loss is computed using perturbative QCD and considering both elastic and inelastic partonic collisions and path length fluctuations. The approach of Aichelin et al. [83, 84] includes a contribution of radiative gluon emission in the interaction of heavy quarks with light quarks, which are considered as dynamical scattering centers. In this model the relative contribution to the energy loss by radiative processes, as compared to collisional ones, is influenced by introducing a finite gluon mass. The results of the model shown in figure 8, which are obtained for the centrality range 0–50%, correspond to either a pure collisional scenario or a combination of collisional and radiative energy loss. Finally, in the model of Horowitz and Gyulassy [85], also applied to the centrality interval 0–50%, the string inspired AdS/CFT gravity-gauge theory correspondence [86, 87] is applied to the case of heavy quark energy loss. In the right hand inset of figure 8, the ALICE $R_{\rm AA}$ value, integrated over the range $4.5 < p_{\rm T} < 10\,{\rm GeV}/c$, is compared to theoretical predictions computed in the same $p_{\rm T}$ range. Most of the models predict a larger value of $R_{\rm AA}$ than observed in the measurement. However, more precise data are needed to discriminate among the different models. The next LHC run will provide increased statistics for this measurement.

4 Conclusions

A study of J/ψ production at mid-rapidity in Pb-Pb collisions at $\sqrt{s_{\rm NN}} = 2.76\,{\rm TeV}$ has been presented. A reduction of the inclusive J/ψ $\langle p_{\rm T}\rangle$ is observed in Pb-Pb collisions in comparison to pp. The ratio $r_{\rm AA} = \langle p_{\rm T}^2\rangle_{\rm AA}/\langle p_{\rm T}^2\rangle_{\rm pp}$ is found to be significantly below unity, corresponding to a medium-induced change in the shape of the $p_{\rm T}$ spectra. The nuclear modification factor $R_{\rm AA}$ depends on $p_{\rm T}$. It is around 0.8 for $p_{\rm T} < 2.5\,{\rm GeV}/c$ and reaches, at higher $p_{\rm T}$, almost the same level of suppression as observed at RHIC energies at low $p_{\rm T}$. These observations might be indicative of a sizable contribution of charm quark coalescence to the J/ψ production at low $p_{\rm T}$. Transport models including this additional component are able to qualitatively describe the features seen in the data.

The fraction of J/ψ from beauty hadron decays is determined as a function of centrality and $p_{\rm T}$. No significant centrality dependence is observed. By combining this measurement with the inclusive J/ψ results the $R_{\rm AA}$ of non-prompt J/ψ is obtained in the region $1.5 < p_{\rm T} < 10\,{\rm GeV}/c$, thus extending the coverage of CMS to the low $p_{\rm T}$ region. The nuclear modification in the region $4.5 < p_{\rm T} < 10\,{\rm GeV}/c$ is found to be stronger than predicted by most of the models.

JHEP07(2015)051

Acknowledgments

The ALICE Collaboration would like to thank all its engineers and technicians for their invaluable contributions to the construction of the experiment and the CERN accelerator teams for the outstanding performance of the LHC complex. The ALICE Collaboration gratefully acknowledges the resources and support provided by all Grid centres and the Worldwide LHC Computing Grid (WLCG) collaboration. The ALICE Collaboration acknowledges the following funding agencies for their support in building and running the ALICE detector: State Committee of Science, World Federation of Scientists (WFS) and Swiss Fonds Kidagan, Armenia, Conselho Nacional de Desenvolvimento Científico e Tecnológico (CNPq), Financiadora de Estudos e Projetos (FINEP), Fundação de Amparo à Pesquisa do Estado de São Paulo (FAPESP); National Natural Science Foundation of China (NSFC), the Chinese Ministry of Education (CMOE) and the Ministry of Science and Technology of China (MSTC); Ministry of Education and Youth of the Czech Republic; Danish Natural Science Research Council, the Carlsberg Foundation and the Danish National Research Foundation; The European Research Council under the European Community's Seventh Framework Programme; Helsinki Institute of Physics and the Academy of Finland; French CNRS-IN2P3, the 'Region Pays de Loire', 'Region Alsace', 'Region Auvergne' and CEA, France; German Bundesministerium fur Bildung, Wissenschaft, Forschung und Technologie (BMBF) and the Helmholtz Association; General Secretariat for Research and Technology, Ministry of Development, Greece; Hungarian Orszagos Tudomanyos Kutatasi Alappgrammok (OTKA) and National Office for Research and Technology (NKTH); Department of Atomic Energy and Department of Science and Technology of the Government of India; Istituto Nazionale di Fisica Nucleare (INFN) and Centro Fermi - Museo Storico della Fisica e Centro Studi e Ricerche "Enrico Fermi", Italy; MEXT Grant-in-Aid for Specially Promoted Research, Japan; Joint Institute for Nuclear Research, Dubna; National Research Foundation of Korea (NRF); Consejo Nacional de Cienca y Tecnologia (CONACYT), Direccion General de Asuntos del Personal Academico(DGAPA), México, Amerique Latine Formation academique – European Commission(ALFA-EC) and the EPLANET Program (European Particle Physics Latin American Network) Stichting voor Fundamenteel Onderzoek der Materie (FOM) and the Nederlandse Organisatie voor Wetenschappelijk Onderzoek (NWO), Netherlands; Research Council of Norway (NFR); National Science Centre, Poland; Ministry of National Education/Institute for Atomic Physics and Consiliul Naţional al Cercetării Ştiintifice – Executive Agency for Higher Education Research Development and Innovation Funding (CNCS-UEFISCDI) – Romania; Ministry of Education and Science of Russian Federation, Russian Academy of Sciences, Russian Federal Agency of Atomic Energy, Russian Federal Agency for Science and Innovations and The Russian Foundation for Basic Research; Ministry of Education of Slovakia; Department of Science and Technology, South Africa; Centro de Investigaciones Energeticas, Medioambientales y Tecnologicas (CIEMAT), E-Infrastructure shared between Europe and Latin America (EELA), Ministerio de Economía y Competitividad (MINECO) of Spain, Xunta de Galicia (Consellería de Educación), Centro de Aplicaciones Tecnológicas y Desarrollo Nuclear (CEADEN), Cubaenergía, Cuba, and IAEA (International Atomic Energy Agency); Swedish

JHEP07(2015)051

Research Council (VR) and Knut & Alice Wallenberg Foundation (KAW); Ukraine Ministry of Education and Science; United Kingdom Science and Technology Facilities Council (STFC); The United States Department of Energy, the United States National Science Foundation, the State of Texas, and the State of Ohio; Ministry of Science, Education and Sports of Croatia and Unity through Knowledge Fund, Croatia. Council of Scientific and Industrial Research (CSIR), New Delhi, India

References

[1] F. Karsch, *Lattice simulations of the thermodynamics of strongly interacting elementary particles and the exploration of new phases of matter in relativistic heavy ion collisions*, *J. Phys. Conf. Ser.* **46** (2006) 122 [hep-lat/0608003] [INSPIRE].

[2] Wuppertal-Budapest collaboration, S. Borsányi et al., *Is there still any T_c mystery in lattice QCD? Results with physical masses in the continuum limit III*, *JHEP* **09** (2010) 073 [arXiv:1005.3508] [INSPIRE].

[3] S. Borsányi et al., *The QCD equation of state with dynamical quarks*, *JHEP* **11** (2010) 077 [arXiv:1007.2580] [INSPIRE].

[4] A. Bazavov et al., *The chiral and deconfinement aspects of the QCD transition*, *Phys. Rev.* **D 85** (2012) 054503 [arXiv:1111.1710] [INSPIRE].

[5] T. Matsui and H. Satz, *J/ψ Suppression by Quark-Gluon Plasma Formation*, *Phys. Lett.* **B 178** (1986) 416 [INSPIRE].

[6] NA50 collaboration, B. Alessandro et al., *A new measurement of J/ψ suppression in Pb-Pb collisions at 158-GeV per nucleon*, *Eur. Phys. J.* **C 39** (2005) 335 [hep-ex/0412036] [INSPIRE].

[7] NA60 collaboration, R. Arnaldi, *J/ψ production in p-A and A-A collisions at fixed target experiments*, *Nucl. Phys.* **A 830** (2009) 345C–352C [arXiv:0907.5004] [INSPIRE].

[8] N. Brambilla et al., *Heavy quarkonium: progress, puzzles and opportunities*, *Eur. Phys. J.* **C 71** (2011) 1534 [arXiv:1010.5827] [INSPIRE].

[9] PHENIX collaboration, A. Adare et al., *J/ψ Production vs Centrality, Transverse Momentum and Rapidity in Au+Au Collisions at $\sqrt{s_{NN}} = 200$ GeV*, *Phys. Rev. Lett.* **98** (2007) 232301 [nucl-ex/0611020] [INSPIRE].

[10] PHENIX collaboration, A. Adare et al., *J/ψ suppression at forward rapidity in Au+Au collisions at $\sqrt{s_{NN}} = 200$ GeV*, *Phys. Rev.* **C 84** (2011) 054912 [arXiv:1103.6269] [INSPIRE].

[11] ALICE collaboration, *J/ψ suppression at forward rapidity in Pb-Pb collisions at $\sqrt{s_{NN}} = 2.76$ TeV*, *Phys. Rev. Lett.* **109** (2012) 072301 [arXiv:1202.1383] [INSPIRE].

[12] ALICE collaboration, *Centrality, rapidity and transverse momentum dependence of J/ψ suppression in Pb-Pb collisions at $\sqrt{s_{\rm NN}} = 2.76$ TeV*, *Phys. Lett.* **B 734** (2014) 314 [arXiv:1311.0214] [INSPIRE].

[13] CMS collaboration, *Suppression of non-prompt J/ψ, prompt J/ψ and Y(1S) in PbPb collisions at $\sqrt{s_{NN}} = 2.76$ TeV*, JHEP **05** (2012) 063 [arXiv:1201.5069] [INSPIRE].

[14] P. Braun-Munzinger and J. Stachel, *(Non)thermal aspects of charmonium production and a new look at J/ψ suppression*, Phys. Lett. **B 490** (2000) 196 [nucl-th/0007059] [INSPIRE].

[15] R.L. Thews, M. Schroedter and J. Rafelski, *Enhanced J/ψ production in deconfined quark matter*, Phys. Rev. **C 63** (2001) 054905 [hep-ph/0007323] [INSPIRE].

[16] M.I. Gorenstein, A.P. Kostyuk, H. Stoecker and W. Greiner, *Statistical coalescence model with exact charm conservation*, Phys. Lett. **B 509** (2001) 277 [hep-ph/0010148] [INSPIRE].

[17] A. Andronic, P. Braun-Munzinger, K. Redlich and J. Stachel, *Statistical hadronization of charm in heavy ion collisions at SPS, RHIC and LHC*, Phys. Lett. **B 571** (2003) 36 [nucl-th/0303036] [INSPIRE].

[18] X. Zhao and R. Rapp, *Transverse Momentum Spectra of J/ψ in Heavy-Ion Collisions*, Phys. Lett. **B 664** (2008) 253 [arXiv:0712.2407] [INSPIRE].

[19] Y.-p. Liu, Z. Qu, N. Xu and P.-f. Zhuang, *J/ψ Transverse Momentum Distribution in High Energy Nuclear Collisions at RHIC*, Phys. Lett. **B 678** (2009) 72 [arXiv:0901.2757] [INSPIRE].

[20] ALICE collaboration, *J/ψ Elliptic Flow in Pb-Pb Collisions at $\sqrt{s_{\mathrm{NN}}} = 2.76$ TeV*, Phys. Rev. Lett. **111** (2013) 162301 [arXiv:1303.5880] [INSPIRE].

[21] M. Gyulassy and M. Plumer, *Jet Quenching in Dense Matter*, Phys. Lett. **B 243** (1990) 432 [INSPIRE].

[22] R. Baier, Y.L. Dokshitzer, A.H. Mueller, S. Peigne and D. Schiff, *Radiative energy loss and p_T broadening of high-energy partons in nuclei*, Nucl. Phys. **B 484** (1997) 265 [hep-ph/9608322] [INSPIRE].

[23] M.H. Thoma and M. Gyulassy, *Quark Damping and Energy Loss in the High Temperature QCD*, Nucl. Phys. **B 351** (1991) 491 [INSPIRE].

[24] E. Braaten and M.H. Thoma, *Energy loss of a heavy fermion in a hot plasma*, Phys. Rev. **D 44** (1991) 1298 [INSPIRE].

[25] E. Braaten and M.H. Thoma, *Energy loss of a heavy quark in the quark-gluon plasma*, Phys. Rev. **D 44** (1991) 2625 [INSPIRE].

[26] Y.L. Dokshitzer and D.E. Kharzeev, *Heavy quark colorimetry of QCD matter*, Phys. Lett. **B 519** (2001) 199 [hep-ph/0106202] [INSPIRE].

[27] N. Armesto, C.A. Salgado and U.A. Wiedemann, *Medium induced gluon radiation off massive quarks fills the dead cone*, Phys. Rev. **D 69** (2004) 114003 [hep-ph/0312106] [INSPIRE].

[28] S. Wicks, W. Horowitz, M. Djordjevic and M. Gyulassy, *Heavy quark jet quenching with collisional plus radiative energy loss and path length fluctuations*, Nucl. Phys. **A 783** (2007) 493 [nucl-th/0701063] [INSPIRE].

[29] B.-W. Zhang, E. Wang and X.-N. Wang, *Heavy quark energy loss in nuclear medium*, Phys. Rev. Lett. **93** (2004) 072301 [nucl-th/0309040] [INSPIRE].

[30] R. Sharma, I. Vitev and B.-W. Zhang, *Light-cone wave function approach to open heavy flavor dynamics in QCD matter*, Phys. Rev. **C 80** (2009) 054902 [arXiv:0904.0032] [INSPIRE].

[31] R. Sharma and I. Vitev, *High transverse momentum quarkonium production and dissociation in heavy ion collisions*, Phys. Rev. **C 87** (2013) 044905 [arXiv:1203.0329] [INSPIRE].

JHEP07(2015)051

[32] A. Adil and I. Vitev, *Collisional dissociation of heavy mesons in dense QCD matter*, *Phys. Lett.* **B 649** (2007) 139 [hep-ph/0611109] [INSPIRE].

[33] P. Faccioli, C. Lourenco, J. Seixas and H.K. Woehri, *Study of ψ' and χ_c decays as feed-down sources of J/ψ hadro-production*, *JHEP* **10** (2008) 004 [arXiv:0809.2153] [INSPIRE].

[34] A. Mócsy and P. Petreczky, *Color screening melts quarkonium*, *Phys. Rev. Lett.* **99** (2007) 211602 [arXiv:0706.2183] [INSPIRE].

[35] ATLAS collaboration, *Measurement of the differential cross-sections of inclusive, prompt and non-prompt J/ψ production in proton-proton collisions at $\sqrt{s} = 7$ TeV*, *Nucl. Phys.* **B 850** (2011) 387 [arXiv:1104.3038] [INSPIRE].

[36] CMS collaboration, *J/ψ and $\psi(2S)$ production in pp collisions at $\sqrt{s} = 7$ TeV*, *JHEP* **02** (2012) 011 [arXiv:1111.1557] [INSPIRE].

[37] ALICE collaboration, *Measurement of prompt J/ψ and beauty hadron production cross sections at mid-rapidity in pp collisions at $\sqrt{s} = 7$ TeV*, *JHEP* **11** (2012) 065 [arXiv:1205.5880] [INSPIRE].

[38] ALICE collaboration, *The ALICE experiment at the CERN LHC*, 2008 *JINST* **3** S08002 [INSPIRE].

[39] ALICE collaboration, *Alignment of the ALICE Inner Tracking System with cosmic-ray tracks*, 2010 *JINST* **5** P03003 [arXiv:1001.0502] [INSPIRE].

[40] J. Alme et al., *The ALICE TPC, a large 3-dimensional tracking device with fast readout for ultra-high multiplicity events*, *Nucl. Instrum. Meth.* **A 622** (2010) 316 [arXiv:1001.1950] [INSPIRE].

[41] ALICE collaboration, *Performance of the ALICE VZERO system*, 2013 *JINST* **8** P10016 [arXiv:1306.3130] [INSPIRE].

[42] ALICE collaboration, *Measurement of the Cross Section for Electromagnetic Dissociation with Neutron Emission in Pb-Pb Collisions at $\sqrt{s_{NN}} = 2.76$ TeV*, *Phys. Rev. Lett.* **109** (2012) 252302 [arXiv:1203.2436] [INSPIRE].

[43] ALICE collaboration, *Centrality determination of Pb-Pb collisions at $\sqrt{s_{NN}} = 2.76$ TeV with ALICE*, *Phys. Rev.* **C 88** (2013) 044909 [arXiv:1301.4361] [INSPIRE].

[44] ALICE collaboration, *Rapidity and transverse momentum dependence of inclusive J/ψ production in pp collisions at $\sqrt{s} = 7$ TeV*, *Phys. Lett.* **B 704** (2011) 442 [arXiv:1105.0380] [INSPIRE].

[45] ALICE collaboration, *Performance of the ALICE Experiment at the CERN LHC*, *Int. J. Mod. Phys.* **A 29** (2014) 1430044 [arXiv:1402.4476] [INSPIRE].

[46] ALICE collaboration, *J/ψ polarization in pp collisions at $\sqrt{s} = 7$ TeV*, *Phys. Rev. Lett.* **108** (2012) 082001 [arXiv:1111.1630] [INSPIRE].

[47] CMS collaboration, *Measurement of the prompt J/ψ and ψ(2S) polarizations in pp collisions at $\sqrt{s} = 7$ TeV*, *Phys. Lett.* **B 727** (2013) 381 [arXiv:1307.6070] [INSPIRE].

[48] LHCb collaboration, *Measurement of J/ψ polarization in pp collisions at $\sqrt{s} = 7$ TeV*, *Eur. Phys. J.* **C 73** (2013) 2631 [arXiv:1307.6379] [INSPIRE].

[49] X.-N. Wang and M. Gyulassy, *HIJING: A Monte Carlo model for multiple jet production in p p, p A and A A collisions*, *Phys. Rev.* **D 44** (1991) 3501 [INSPIRE].

[50] F. Bossu et al., *Phenomenological interpolation of the inclusive J/ψ cross section to proton-proton collisions at 2.76 TeV and 5.5 TeV*, arXiv:1103.2394 [INSPIRE].

[51] K.J. Eskola, V.J. Kolhinen and C.A. Salgado, *The Scale dependent nuclear effects in parton distributions for practical applications*, Eur. Phys. J. **C 9** (1999) 61 [hep-ph/9807297] [INSPIRE].

[52] D.J. Lange, *The EvtGen particle decay simulation package*, Nucl. Instrum. Meth. **A 462** (2001) 152 [INSPIRE].

[53] E. Barberio and Z. Was, *PHOTOS: A Universal Monte Carlo for QED radiative corrections. Version 2.0*, Comput. Phys. Commun. **79** (1994) 291 [INSPIRE].

[54] R. Brun, F. Carminati and S. Giani, *GEANT Detector Description and Simulation Tool*, CERN-W5013, CERN-W-5013 (1994).

[55] ALICE collaboration, *Inclusive J/ψ production in pp collisions at $\sqrt{s} = 2.76$ TeV*, Phys. Lett. **B 718** (2012) 295 [arXiv:1203.3641] [INSPIRE].

[56] PHENIX collaboration, A. Adare et al., *J/ψ production versus transverse momentum and rapidity in p^+p collisions at $\sqrt{s}$ = 200-GeV*, Phys. Rev. Lett. **98** (2007) 232002 [hep-ex/0611020] [INSPIRE].

[57] CDF collaboration, *Measurement of the J/ψ meson and $b-$hadron production cross sections in $p\bar{p}$ collisions at $\sqrt{s} = 1960$ GeV*, Phys. Rev. **D 71** (2005) 032001 [hep-ex/0412071] [INSPIRE].

[58] Particle Data Group collaboration, K. Olive et al., *Review of Particle Physics*, Chin. Phys. **C 38** (2014) 090001.

[59] W.M. Alberico et al., *Heavy-flavour spectra in high energy nucleus-nucleus collisions*, Eur. Phys. J. **C 71** (2011) 1666 [arXiv:1101.6008] [INSPIRE].

[60] W.M. Alberico, et al., *Heavy flavors in AA collisions: production, transport and final spectra*, Eur. Phys. J. **C 73** (2013) 2481 [arXiv:1305.7421] [INSPIRE].

[61] J. Uphoff, O. Fochler, Z. Xu and C. Greiner, *Open Heavy Flavor in Pb+Pb Collisions at $\sqrt{s} = 2.76$ TeV within a Transport Model*, Phys. Lett. **B 717** (2012) 430 [arXiv:1205.4945] [INSPIRE].

[62] BaBar collaboration, B. Aubert et al., *Study of inclusive production of charmonium mesons in B decay*, Phys. Rev. **D 67** (2003) 032002 [hep-ex/0207097] [INSPIRE].

[63] LHCb collaboration, *Measurement of J/ψ production in pp collisions at $\sqrt{s} = 7$ TeV*, Eur. Phys. J. **C 71** (2011) 1645 [arXiv:1103.0423] [INSPIRE].

[64] CDF collaboration, *Polarization of J/ψ and ψ_{2S} mesons produced in $p\bar{p}$ collisions at $\sqrt{s} = 1.96$-TeV*, Phys. Rev. Lett. **99** (2007) 132001 [arXiv:0704.0638] [INSPIRE].

[65] ALICE collaboration, *Suppression of high transverse momentum D mesons in central Pb-Pb collisions at $\sqrt{s_{NN}} = 2.76$ TeV*, JHEP **09** (2012) 112 [arXiv:1203.2160] [INSPIRE].

[66] ALICE collaboration, *Technical Design Report for the Upgrade of the ALICE Inner Tracking System*, J. Phys. **G 41** (2014) 087002 [INSPIRE].

[67] T. Sjöstrand, S. Mrenna and P.Z. Skands, *PYTHIA 6.4 Physics and Manual*, JHEP **05** (2006) 026 [hep-ph/0603175] [INSPIRE].

[68] P.Z. Skands, *Tuning Monte Carlo Generators: The Perugia Tunes*, Phys. Rev. **D 82** (2010) 074018 [arXiv:1005.3457] [INSPIRE].

[69] ALICE collaboration, K. Koch, *π^0 and η measurement with photon conversions in ALICE in proton-proton collisions at $\sqrt{s} = 7$ TeV*, Nucl. Phys. **A 855** (2011) 281 [arXiv:1103.2217] [INSPIRE].

[70] CMS collaboration, *Prompt and non-prompt J/ψ production in pp collisions at $\sqrt{s} = 7$ TeV*, Eur. Phys. J. **C 71** (2011) 1575 [arXiv:1011.4193] [INSPIRE].

[71] M. Cacciari et al., *Theoretical predictions for charm and bottom production at the LHC*, JHEP **10** (2012) 137 [arXiv:1205.6344] [INSPIRE].

[72] PHENIX collaboration, A. Adare et al., *J/ψ Production in $\sqrt{s_{NN}} = 200$ GeV Cu+Cu Collisions*, Phys. Rev. Lett. **101** (2008) 122301 [arXiv:0801.0220] [INSPIRE].

[73] NA50 collaboration, M.C. Abreu et al., *Transverse momentum distributions of J/ψ, ψ′, Drell-Yan and continuum dimuons produced in Pb Pb interactions at the SPS*, Phys. Lett. **B 499** (2001) 85 [INSPIRE].

[74] K. Zhou, N. Xu, Z. Xu and P. Zhuang, *Medium effects on charmonium production at ultrarelativistic energies available at the CERN Large Hadron Collider*, Phys. Rev. **C 89** (2014) 054911 [arXiv:1401.5845] [INSPIRE].

[75] X. Zhao and R. Rapp, *Charmonium in Medium: From Correlators to Experiment*, Phys. Rev. **C 82** (2010) 064905 [arXiv:1008.5328] [INSPIRE].

[76] X. Zhao and R. Rapp, *Medium Modifications and Production of Charmonia at LHC*, Nucl. Phys. **A 859** (2011) 114 [arXiv:1102.2194] [INSPIRE].

[77] K. Zhou, N. Xu and P. Zhuang, *Quarkonium Production and Medium Effects in High Energy Nuclear Collisions*, arXiv:1309.7520 [INSPIRE].

[78] K. Tuchin, *Forward hadron production in high energy pA collisions: From RHIC to LHC*, Nucl. Phys. **A 798** (2008) 61 [arXiv:0705.2193] [INSPIRE].

[79] ALICE collaboration, *Differential studies of J/ψ and ψ(2S) production in Pb-Pb collisions at $\sqrt{s_{NN}} = 2.76$ TeV*, arXiv:1506.08804.

[80] M. He, R.J. Fries and R. Rapp, *Heavy Flavor at the Large Hadron Collider in a Strong Coupling Approach*, Phys. Lett. **B 735** (2014) 445 [arXiv:1401.3817] [INSPIRE].

[81] M. Djordjevic and M. Djordjevic, *LHC jet suppression of light and heavy flavor observables*, Phys. Lett. **B 734** (2014) 286 [arXiv:1307.4098] [INSPIRE].

[82] S. Wicks, W. Horowitz, M. Djordjevic and M. Gyulassy, *Elastic, inelastic and path length fluctuations in jet tomography*, Nucl. Phys. **A 784** (2007) 426 [nucl-th/0512076] [INSPIRE].

[83] J. Aichelin, P.B. Gossiaux and T. Gousset, *Gluon radiation by heavy quarks at intermediate energies*, Phys. Rev. **D 89** (2014) 074018 [arXiv:1307.5270] [INSPIRE].

[84] P.B. Gossiaux et al., *Gluon radiation by heavy quarks at intermediate energies and consequences for the mass hierarchy of energy loss*, Nucl. Phys. **A 931** (2014) 581 [arXiv:1409.0900] [INSPIRE].

[85] W.A. Horowitz and M. Gyulassy, *Heavy quark jet tomography of Pb + Pb at LHC: AdS/CFT drag or pQCD energy loss?*, Phys. Lett. **B 666** (2008) 320 [arXiv:0706.2336] [INSPIRE].

[86] J.M. Maldacena, *The Large-N limit of superconformal field theories and supergravity*, Int. J. Theor. Phys. **38** (1999) 1113 [hep-th/9711200] [INSPIRE].

[87] S.S. Gubser, I.R. Klebanov and A.M. Polyakov, *Gauge theory correlators from noncritical string theory*, Phys. Lett. **B 428** (1998) 105 [hep-th/9802109] [INSPIRE].

The ALICE collaboration

J. Adam[40] , D. Adamová[83] , M.M. Aggarwal[87] , G. Aglieri Rinella[36] , M. Agnello[111] , N. Agrawal[48] , Z. Ahammed[132] , S.U. Ahn[68] , I. Aimo[94 ,111] , S. Aiola[137] , M. Ajaz[16] , A. Akindinov[58] , S.N. Alam[132] , D. Aleksandrov[100] , B. Alessandro[111] , D. Alexandre[102] , R. Alfaro Molina[64] , A. Alici[105 ,12] , A. Alkin[3] , J. Alme[38] , T. Alt[43] , S. Altinpinar[18] , I. Altsybeev[131] , C. Alves Garcia Prado[120] , C. Andrei[78] , A. Andronic[97] , V. Anguelov[93] , J. Anielski[54] , T. Antičić[98] , F. Antinori[108] , P. Antonioli[105] , L. Aphecetche[113] , H. Appelshäuser[53] , S. Arcelli[28] , N. Armesto[17] , R. Arnaldi[111] , I.C. Arsene[22] , M. Arslandok[53] , B. Audurier[113] , A. Augustinus[36] , R. Averbeck[97] , M.D. Azmi[19] , M. Bach[43] , A. Badalà[107] , Y.W. Baek[44] , S. Bagnasco[111] , R. Bailhache[53] , R. Bala[90] , A. Baldisseri[15] , F. Baltasar Dos Santos Pedrosa[36] , R.C. Baral[61] , A.M. Barbano[111] , R. Barbera[29] , F. Barile[33] , G.G. Barnaföldi[136] , L.S. Barnby[102] , V. Barret[70] , P. Bartalini[7] , K. Barth[36] , J. Bartke[117] , E. Bartsch[53] , M. Basile[28] , N. Bastid[70] , S. Basu[132] , B. Bathen[54] , G. Batigne[113] , A. Batista Camejo[70] , B. Batyunya[66] , P.C. Batzing[22] , I.G. Bearden[80] , H. Beck[53] , C. Bedda[111] , N.K. Behera[49 ,48] , I. Belikov[55] , F. Bellini[28] , H. Bello Martinez[2] , R. Bellwied[122] , R. Belmont[135] , E. Belmont-Moreno[64] , V. Belyaev[76] , G. Bencedi[136] , S. Beole[27] , I. Berceanu[78] , A. Bercuci[78] , Y. Berdnikov[85] , D. Berenyi[136] , R.A. Bertens[57] , D. Berzano[36 ,27] , L. Betev[36] , A. Bhasin[90] , I.R. Bhat[90] , A.K. Bhati[87] , B. Bhattacharjee[45] , J. Bhom[128] , L. Bianchi[122] , N. Bianchi[72] , C. Bianchin[135 ,57] , J. Bielčík[40] , J. Bielčíková[83] , A. Bilandzic[80] , R. Biswas[4] , S. Biswas[79] , S. Bjelogrlic[57] , F. Blanco[10] , D. Blau[100] , C. Blume[53] , F. Bock[74 ,93] , A. Bogdanov[76] , H. Bøggild[80] , L. Boldizsár[136] , M. Bombara[41] , J. Book[53] , H. Borel[15] , A. Borissov[96] , M. Borri[82] , F. Bossú[65] , M. Botje[81] , E. Botta[27] , S. Böttger[52] , P. Braun-Munzinger[97] , M. Bregant[120] , T. Breitner[52] , T.A. Broker[53] , T.A. Browning[95] , M. Broz[40] , E.J. Brucken[46] , E. Bruna[111] , G.E. Bruno[33] , D. Budnikov[99] , H. Buesching[53] , S. Bufalino[111 ,36] , P. Buncic[36] , O. Busch[93 ,128] , Z. Buthelezi[65] , J.T. Buxton[20] , D. Caffarri[36] , X. Cai[7] , H. Caines[137] , L. Calero Diaz[72] , A. Caliva[57] , E. Calvo Villar[103] , P. Camerini[26] , F. Carena[36] , W. Carena[36] , J. Castillo Castellanos[15] , A.J. Castro[125] , E.A.R. Casula[25] , C. Cavicchioli[36] , C. Ceballos Sanchez[9] , J. Cepila[40] , P. Cerello[111] , J. Cerkala[115] , B. Chang[123] , S. Chapeland[36] , M. Chartier[124] , J.L. Charvet[15] , S. Chattopadhyay[132] , S. Chattopadhyay[101] , V. Chelnokov[3] , M. Cherney[86] , C. Cheshkov[130] , B. Cheynis[130] , V. Chibante Barroso[36] , D.D. Chinellato[121] , P. Chochula[36] , K. Choi[96] , M. Chojnacki[80] , S. Choudhury[132] , P. Christakoglou[81] , C.H. Christensen[80] , P. Christiansen[34] , T. Chujo[128] , S.U. Chung[96] , Z. Chunhui[57] , C. Cicalo[106] , L. Cifarelli[12 ,28] , F. Cindolo[105] , J. Cleymans[89] , F. Colamaria[33] , D. Colella[33] , A. Collu[25] , M. Colocci[28] , G. Conesa Balbastre[71] , Z. Conesa del Valle[51] , M.E. Connors[137] , J.G. Contreras[11 ,40] , T.M. Cormier[84] , Y. Corrales Morales[27] , I. Cortés Maldonado[2] , P. Cortese[32] , M.R. Cosentino[120] , F. Costa[36] , P. Crochet[70] , R. Cruz Albino[11] , E. Cuautle[63] , L. Cunqueiro[36] , T. Dahms[92 ,37] , A. Dainese[108] , A. Danu[62] , D. Das[101] , I. Das[51 ,101] , S. Das[4] , A. Dash[121] , S. Dash[48] , S. De[120] , A. De Caro[31 ,12] , G. de Cataldo[104] , J. de Cuveland[43] , A. De Falco[25] , D. De Gruttola[12 ,31] , N. De Marco[111] , S. De Pasquale[31] , A. Deisting[97 ,93] , A. Deloff[77] , E. Dénes[136] , G. D'Erasmo[33] , D. Di Bari[33] , A. Di Mauro[36] , P. Di Nezza[72] , M.A. Diaz Corchero[10] , T. Dietel[89] , P. Dillenseger[53] , R. Divià[36] , Ø. Djuvsland[18] , A. Dobrin[57 ,81] , T. Dobrowolski[77 ,i] , D. Domenicis Gimenez[120] , B. Dönigus[53] , O. Dordic[22] , A.K. Dubey[132] , A. Dubla[57] , L. Ducroux[130] , P. Dupieux[70] , R.J. Ehlers[137] , D. Elia[104] , H. Engel[52] , B. Erazmus[36 ,113] , I. Erdemir[53] , F. Erhardt[129] , D. Eschweiler[43] , B. Espagnon[51] , M. Estienne[113] , S. Esumi[128] , J. Eum[96] , D. Evans[102] , S. Evdokimov[112] , G. Eyyubova[40] , L. Fabbietti[37 ,92] , D. Fabris[108] , J. Faivre[71] , A. Fantoni[72] , M. Fasel[74] , L. Feldkamp[54] , D. Felea[62] , A. Feliciello[111] , G. Feofilov[131] , J. Ferencei[83] , A. Fernández Téllez[2] , E.G. Ferreiro[17] ,

A. Ferretti[27] , A. Festanti[30] , V.J.G. Feuillard[15] , J. Figiel[117] , M.A.S. Figueredo[124] , S. Filchagin[99] , D. Finogeev[56] , F.M. Fionda[104] , E.M. Fiore[33] , M.G. Fleck[93] , M. Floris[36] , S. Foertsch[65] , P. Foka[97] , S. Fokin[100] , E. Fragiacomo[110] , A. Francescon[36 ,30] , U. Frankenfeld[97] , U. Fuchs[36] , C. Furget[71] , A. Furs[56] , M. Fusco Girard[31] , J.J. Gaardhøje[80] , M. Gagliardi[27] , A.M. Gago[103] , M. Gallio[27] , D.R. Gangadharan[74] , P. Ganoti[88] , C. Gao[7] , C. Garabatos[97] , E. Garcia-Solis[13] , C. Gargiulo[36] , P. Gasik[92 ,37] , M. Germain[113] , A. Gheata[36] , M. Gheata[62 ,36] , P. Ghosh[132] , S.K. Ghosh[4] , P. Gianotti[72] , P. Giubellino[36] , P. Giubilato[30] , E. Gladysz-Dziadus[117] , P. Glässel[93] , A. Gomez Ramirez[52] , P. González-Zamora[10] , S. Gorbunov[43] , L. Görlich[117] , S. Gotovac[116] , V. Grabski[64] , L.K. Graczykowski[134] , K.L. Graham[102] , A. Grelli[57] , A. Grigoras[36] , C. Grigoras[36] , V. Grigoriev[76] , A. Grigoryan[1] , S. Grigoryan[66] , B. Grinyov[3] , N. Grion[110] , J.F. Grosse-Oetringhaus[36] , J.-Y. Grossiord[130] , R. Grosso[36] , F. Guber[56] , R. Guernane[71] , B. Guerzoni[28] , K. Gulbrandsen[80] , H. Gulkanyan[1] , T. Gunji[127] , A. Gupta[90] , R. Gupta[90] , R. Haake[54] , Ø. Haaland[18] , C. Hadjidakis[51] , M. Haiduc[62] , H. Hamagaki[127] , G. Hamar[136] , A. Hansen[80] , J.W. Harris[137] , H. Hartmann[43] , A. Harton[13] , D. Hatzifotiadou[105] , S. Hayashi[127] , S.T. Heckel[53] , M. Heide[54] , H. Helstrup[38] , A. Herghelegiu[78] , G. Herrera Corral[11] , B.A. Hess[35] , K.F. Hetland[38] , T.E. Hilden[46] , H. Hillemanns[36] , B. Hippolyte[55] , P. Hristov[36] , M. Huang[18] , T.J. Humanic[20] , N. Hussain[45] , T. Hussain[19] , D. Hutter[43] , D.S. Hwang[21] , R. Ilkaev[99] , I. Ilkiv[77] , M. Inaba[128] , C. Ionita[36] , M. Ippolitov[76 ,100] , M. Irfan[19] , M. Ivanov[97] , V. Ivanov[85] , V. Izucheev[112] , P.M. Jacobs[74] , S. Jadlovska[115] , C. Jahnke[120] , H.J. Jang[68] , M.A. Janik[134] , P.H.S.Y. Jayarathna[122] , C. Jena[30] , S. Jena[122] , R.T. Jimenez Bustamante[97] , P.G. Jones[102] , H. Jung[44] , A. Jusko[102] , P. Kalinak[59] , A. Kalweit[36] , J. Kamin[53] , J.H. Kang[138] , V. Kaplin[76] , S. Kar[132] , A. Karasu Uysal[69] , O. Karavichev[56] , T. Karavicheva[56] , E. Karpechev[56] , U. Kebschull[52] , R. Keidel[139] , D.L.D. Keijdener[57] , M. Keil[36] , K.H. Khan[16] , M.M. Khan[19] , P. Khan[101] , S.A. Khan[132] , A. Khanzadeev[85] , Y. Kharlov[112] , B. Kileng[38] , B. Kim[138] , D.W. Kim[68 ,44] , D.J. Kim[123] , H. Kim[138] , J.S. Kim[44] , M. Kim[44] , M. Kim[138] , S. Kim[21] , T. Kim[138] , S. Kirsch[43] , I. Kisel[43] , S. Kiselev[58] , A. Kisiel[134] , G. Kiss[136] , J.L. Klay[6] , C. Klein[53] , J. Klein[93] , C. Klein-Bösing[54] , A. Kluge[36] , M.L. Knichel[93] , A.G. Knospe[118] , T. Kobayashi[128] , C. Kobdaj[114] , M. Kofarago[36] , T. Kollegger[97 ,43] , A. Kolojvari[131] , V. Kondratiev[131] , N. Kondratyeva[76] , E. Kondratyuk[112] , A. Konevskikh[56] , M. Kopcik[115] , C. Kouzinopoulos[36] , O. Kovalenko[77] , V. Kovalenko[131] , M. Kowalski[117] , S. Kox[71] , G. Koyithatta Meethaleveedu[48] , J. Kral[123] , I. Králik[59] , A. Kravčáková[41] , M. Krelina[40] , M. Kretz[43] , M. Krivda[102 ,59] , F. Krizek[83] , E. Kryshen[36] , M. Krzewicki[43] , A.M. Kubera[20] , V. Kučera[83] , T. Kugathasan[36] , C. Kuhn[55] , P.G. Kuijer[81] , I. Kulakov[43] , J. Kumar[48] , L. Kumar[79 ,87] , P. Kurashvili[77] , A. Kurepin[56] , A.B. Kurepin[56] , A. Kuryakin[99] , S. Kushpil[83] , M.J. Kweon[50] , Y. Kwon[138] , S.L. La Pointe[111] , P. La Rocca[29] , C. Lagana Fernandes[120] , I. Lakomov[36] , R. Langoy[42] , C. Lara[52] , A. Lardeux[15] , A. Lattuca[27] , E. Laudi[36] , R. Lea[26] , L. Leardini[93] , G.R. Lee[102] , S. Lee[138] , I. Legrand[36] , R.C. Lemmon[82] , V. Lenti[104] , E. Leogrande[57] , I. León Monzón[119] , M. Leoncino[27] , P. Lévai[136] , S. Li[7 ,70] , X. Li[14] , J. Lien[42] , R. Lietava[102] , S. Lindal[22] , V. Lindenstruth[43] , C. Lippmann[97] , M.A. Lisa[20] , H.M. Ljunggren[34] , D.F. Lodato[57] , P.I. Loenne[18] , V.R. Loggins[135] , V. Loginov[76] , C. Loizides[74] , X. Lopez[70] , E. López Torres[9] , A. Lowe[136] , P. Luettig[53] , M. Lunardon[30] , G. Luparello[26] , P.H.F.N.D. Luz[120] , A. Maevskaya[56] , M. Mager[36] , S. Mahajan[90] , S.M. Mahmood[22] , A. Maire[55] , R.D. Majka[137] , M. Malaev[85] , I. Maldonado Cervantes[63] , L. Malinina[66] , D. Mal'Kevich[58] , P. Malzacher[97] , A. Mamonov[99] , L. Manceau[111] , V. Manko[100] , F. Manso[70] , V. Manzari[104 ,36] , M. Marchisone[27] , J. Mareš[60] , G.V. Margagliotti[26] , A. Margotti[105] , J. Margutti[57] , A. Marín[97] , C. Markert[118] , M. Marquard[53] , N.A. Martin[97] , J. Martin Blanco[113] , P. Martinengo[36] , M.I. Martínez[2] , G. Martínez García[113] , M. Martinez Pedreira[36] , Y. Martynov[3] , A. Mas[120] , S. Masciocchi[97] , M. Masera[27] , A. Masoni[106] , L. Massacrier[113] ,

JHEP07(2015)051

A. Mastroserio[33], H. Masui[128], A. Matyja[117], C. Mayer[117], J. Mazer[125], M.A. Mazzoni[109], D. Mcdonald[122], F. Meddi[24], A. Menchaca-Rocha[64], E. Meninno[31], J. Mercado Pérez[93], M. Meres[39], Y. Miake[128], M.M. Mieskolainen[46], K. Mikhaylov[58,66], L. Milano[36], J. Milosevic[22,133], L.M. Minervini[23,104], A. Mischke[57], A.N. Mishra[49], D. Miśkowiec[97], J. Mitra[132], C.M. Mitu[62], N. Mohammadi[57], B. Mohanty[79,132], L. Molnar[55], L. Montaño Zetina[11], E. Montes[10], M. Morando[30], D.A. Moreira De Godoy[54,113], S. Moretto[30], A. Morreale[113], A. Morsch[36], V. Muccifora[72], E. Mudnic[116], D. Mühlheim[54], S. Muhuri[132], M. Mukherjee[132], J.D. Mulligan[137], M.G. Munhoz[120], S. Murray[65], L. Musa[36], J. Musinsky[59], B.K. Nandi[48], R. Nania[105], E. Nappi[104], M.U. Naru[16], C. Nattrass[125], K. Nayak[79], T.K. Nayak[132], S. Nazarenko[99], A. Nedosekin[58], L. Nellen[63], F. Ng[122], M. Nicassio[97], M. Niculescu[62,36], J. Niedziela[36], B.S. Nielsen[80], S. Nikolaev[100], S. Nikulin[100], V. Nikulin[85], F. Noferini[12,105], P. Nomokonov[66], G. Nooren[57], J. Norman[124], A. Nyanin[100], J. Nystrand[18], H. Oeschler[93], S. Oh[137], S.K. Oh[67], A. Ohlson[36], A. Okatan[69], T. Okubo[47], L. Olah[136], J. Oleniacz[134], A.C. Oliveira Da Silva[120], M.H. Oliver[137], J. Onderwaater[97], C. Oppedisano[111], A. Ortiz Velasquez[63], A. Oskarsson[34], J. Otwinowski[117], K. Oyama[93], M. Ozdemir[53], Y. Pachmayer[93], P. Pagano[31], G. Paić[63], C. Pajares[17], S.K. Pal[132], J. Pan[135], A.K. Pandey[48], D. Pant[48], P. Papcun[115], V. Papikyan[1], G.S. Pappalardo[107], P. Pareek[49], W.J. Park[97], S. Parmar[87], A. Passfeld[54], V. Paticchio[104], R.N. Patra[132], B. Paul[101], T. Peitzmann[57], H. Pereira Da Costa[15], E. Pereira De Oliveira Filho[120], D. Peresunko[76,100], C.E. Pérez Lara[81], V. Peskov[53], Y. Pestov[5], V. Petráček[40], V. Petrov[112], M. Petrovici[78], C. Petta[29], S. Piano[110], M. Pikna[39], P. Pillot[113], O. Pinazza[105,36], L. Pinsky[122], D.B. Piyarathna[122], M. Płoskoń[74], M. Planinic[129], J. Pluta[134], S. Pochybova[136], P.L.M. Podesta-Lerma[119], M.G. Poghosyan[86], B. Polichtchouk[112], N. Poljak[129], W. Poonsawat[114], A. Pop[78], S. Porteboeuf-Houssais[70], J. Porter[74], J. Pospisil[83], S.K. Prasad[4], R. Preghenella[105,36], F. Prino[111], C.A. Pruneau[135], I. Pshenichnov[56], M. Puccio[111], G. Puddu[25], P. Pujahari[135], V. Punin[99], J. Putschke[135], H. Qvigstad[22], A. Rachevski[110], S. Raha[4], S. Rajput[90], J. Rak[123], A. Rakotozafindrabe[15], L. Ramello[32], R. Raniwala[91], S. Raniwala[91], S.S. Räsänen[46], B.T. Rascanu[53], D. Rathee[87], K.F. Read[125], J.S. Real[71], K. Redlich[77], R.J. Reed[135], A. Rehman[18], P. Reichelt[53], F. Reidt[93,36], X. Ren[7], R. Renfordt[53], A.R. Reolon[72], A. Reshetin[56], F. Rettig[43], J.-P. Revol[12], K. Reygers[93], V. Riabov[85], R.A. Ricci[73], T. Richert[34], M. Richter[22], P. Riedler[36], W. Riegler[36], F. Riggi[29], C. Ristea[62], A. Rivetti[111], E. Rocco[57], M. Rodríguez Cahuantzi[2], A. Rodriguez Manso[81], K. Røed[22], E. Rogochaya[66], D. Rohr[43], D. Röhrich[18], R. Romita[124], F. Ronchetti[72], L. Ronflette[113], P. Rosnet[70], A. Rossi[36,30], F. Roukoutakis[88], A. Roy[49], C. Roy[55], P. Roy[101], A.J. Rubio Montero[10], R. Rui[26], R. Russo[27], E. Ryabinkin[100], Y. Ryabov[85], A. Rybicki[117], S. Sadovsky[112], K. Šafařík[36], B. Sahlmuller[53], P. Sahoo[49], R. Sahoo[49], S. Sahoo[61], P.K. Sahu[61], J. Saini[132], S. Sakai[72], M.A. Saleh[135], C.A. Salgado[17], J. Salzwedel[20], S. Sambyal[90], V. Samsonov[85], X. Sanchez Castro[55], L. Šándor[59], A. Sandoval[64], M. Sano[128], G. Santagati[29], D. Sarkar[132], E. Scapparone[105], F. Scarlassara[30], R.P. Scharenberg[95], C. Schiaua[78], R. Schicker[93], C. Schmidt[97], H.R. Schmidt[35], S. Schuchmann[53], J. Schukraft[36], M. Schulc[40], T. Schuster[137], Y. Schutz[113,36], K. Schwarz[97], K. Schweda[97], G. Scioli[28], E. Scomparin[111], R. Scott[125], K.S. Seeder[120], J.E. Seger[86], Y. Sekiguchi[127], D. Sekihata[47], I. Selyuzhenkov[97], K. Senosi[65], J. Seo[96,67], E. Serradilla[64,10], A. Sevcenco[62], A. Shabanov[56], A. Shabetai[113], O. Shadura[3], R. Shahoyan[36], A. Shangaraev[112], A. Sharma[90], N. Sharma[61,125], K. Shigaki[47], K. Shtejer[9,27], Y. Sibiriak[100], S. Siddhanta[106], K.M. Sielewicz[36], T. Siemiarczuk[77], D. Silvermyr[84,34], C. Silvestre[71], G. Simatovic[129], G. Simonetti[36], R. Singaraju[132], R. Singh[79], S. Singha[79,132], V. Singhal[132], B.C. Sinha[132], T. Sinha[101], B. Sitar[39], M. Sitta[32], T.B. Skaali[22], M. Slupecki[123], N. Smirnov[137], R.J.M. Snellings[57], T.W. Snellman[123], C. Søgaard[34], R. Soltz[75], J. Song[96], M. Song[138],

Z. Song[7] , F. Soramel[30] , S. Sorensen[125] , M. Spacek[40] , E. Spiriti[72] , I. Sputowska[117] , M. Spyropoulou-Stassinaki[88] , B.K. Srivastava[95] , J. Stachel[93] , I. Stan[62] , G. Stefanek[77] , M. Steinpreis[20] , E. Stenlund[34] , G. Steyn[65] , J.H. Stiller[93] , D. Stocco[113] , P. Strmen[39] , A.A.P. Suaide[120] , T. Sugitate[47] , C. Suire[51] , M. Suleymanov[16] , R. Sultanov[58] , M. Šumbera[83] , T.J.M. Symons[74] , A. Szabo[39] , A. Szanto de Toledo[120 , i], I. Szarka[39] , A. Szczepankiewicz[36] , M. Szymanski[134] , J. Takahashi[121] , N. Tanaka[128] , M.A. Tangaro[33] , J.D. Tapia Takaki[ii,51] , A. Tarantola Peloni[53] , M. Tarhini[51] , M. Tariq[19] , M.G. Tarzila[78] , A. Tauro[36] , G. Tejeda Muñoz[2] , A. Telesca[36] , K. Terasaki[127] , C. Terrevoli[30 ,25] , B. Teyssier[130] , J. Thäder[74 ,97] , D. Thomas[118] , R. Tieulent[130] , A.R. Timmins[122] , A. Toia[53] , S. Trogolo[111] , V. Trubnikov[3] , W.H. Trzaska[123] , T. Tsuji[127] , A. Tumkin[99] , R. Turrisi[108] , T.S. Tveter[22] , K. Ullaland[18] , A. Uras[130] , G.L. Usai[25] , A. Utrobicic[129] , M. Vajzer[83] , M. Vala[59] , L. Valencia Palomo[70] , S. Vallero[27] , J. Van Der Maarel[57] , J.W. Van Hoorne[36] , M. van Leeuwen[57] , T. Vanat[83] , P. Vande Vyvre[36] , D. Varga[136] , A. Vargas[2] , M. Vargyas[123] , R. Varma[48] , M. Vasileiou[88] , A. Vasiliev[100] , A. Vauthier[71] , V. Vechernin[131] , A.M. Veen[57] , M. Veldhoen[57] , A. Velure[18] , M. Venaruzzo[73] , E. Vercellin[27] , S. Vergara Limón[2] , R. Vernet[8] , M. Verweij[135] , L. Vickovic[116] , G. Viesti[30 , i], J. Viinikainen[123] , Z. Vilakazi[126] , O. Villalobos Baillie[102] , A. Vinogradov[100] , L. Vinogradov[131] , Y. Vinogradov[99] , T. Virgili[31] , V. Vislavicius[34] , Y.P. Viyogi[132] , A. Vodopyanov[66] , M.A. Völkl[93] , K. Voloshin[58] , S.A. Voloshin[135] , G. Volpe[136 ,36] , B. von Haller[36] , I. Vorobyev[92 ,37] , D. Vranic[97 ,36] , J. Vrláková[41] , B. Vulpescu[70] , A. Vyushin[99] , B. Wagner[18] , J. Wagner[97] , H. Wang[57] , M. Wang[7 ,113] , Y. Wang[93] , D. Watanabe[128] , Y. Watanabe[127] , M. Weber[36] , S.G. Weber[97] , J.P. Wessels[54] , U. Westerhoff[54] , J. Wiechula[35] , J. Wikne[22] , M. Wilde[54] , G. Wilk[77] , J. Wilkinson[93] , M.C.S. Williams[105] , B. Windelband[93] , M. Winn[93] , C.G. Yaldo[135] , H. Yang[57] , P. Yang[7] , S. Yano[47] , Z. Yin[7] , H. Yokoyama[128] , I.-K. Yoo[96] , V. Yurchenko[3] , I. Yushmanov[100] , A. Zaborowska[134] , V. Zaccolo[80] , A. Zaman[16] , C. Zampolli[105] , H.J.C. Zanoli[120] , S. Zaporozhets[66] , N. Zardoshti[102] , A. Zarochentsev[131] , P. Závada[60] , N. Zaviyalov[99] , H. Zbroszczyk[134] , I.S. Zgura[62] , M. Zhalov[85] , H. Zhang[18 ,7] , X. Zhang[74] , Y. Zhang[7] , C. Zhao[22] , N. Zhigareva[58] , D. Zhou[7] , Y. Zhou[80 ,57] , Z. Zhou[18] , H. Zhu[18 ,7] , J. Zhu[113 ,7] , X. Zhu[7] , A. Zichichi[12 ,28] , A. Zimmermann[93] , M.B. Zimmermann[54 ,36] , G. Zinovjev[3] , M. Zyzak[43]

[i] *Deceased*

[ii] *Also at: University of Kansas, Lawrence, Kansas, United States*

[1] *A.I. Alikhanyan National Science Laboratory (Yerevan Physics Institute) Foundation, Yerevan, Armenia*

[2] *Benemérita Universidad Autónoma de Puebla, Puebla, Mexico*

[3] *Bogolyubov Institute for Theoretical Physics, Kiev, Ukraine*

[4] *Bose Institute, Department of Physics and Centre for Astroparticle Physics and Space Science (CAPSS), Kolkata, India*

[5] *Budker Institute for Nuclear Physics, Novosibirsk, Russia*

[6] *California Polytechnic State University, San Luis Obispo, California, United States*

[7] *Central China Normal University, Wuhan, China*

[8] *Centre de Calcul de l'IN2P3, Villeurbanne, France*

[9] *Centro de Aplicaciones Tecnológicas y Desarrollo Nuclear (CEADEN), Havana, Cuba*

[10] *Centro de Investigaciones Energéticas Medioambientales y Tecnológicas (CIEMAT), Madrid, Spain*

[11] *Centro de Investigación y de Estudios Avanzados (CINVESTAV), Mexico City and Mérida, Mexico*

[12] *Centro Fermi - Museo Storico della Fisica e Centro Studi e Ricerche "Enrico Fermi", Rome, Italy*

[13] *Chicago State University, Chicago, Illinois, USA*

[14] *China Institute of Atomic Energy, Beijing, China*

JHEP07(2015)051

[15] Commissariat à l'Energie Atomique, IRFU, Saclay, France
[16] COMSATS Institute of Information Technology (CIIT), Islamabad, Pakistan
[17] Departamento de Física de Partículas and IGFAE, Universidad de Santiago de Compostela, Santiago de Compostela, Spain
[18] Department of Physics and Technology, University of Bergen, Bergen, Norway
[19] Department of Physics, Aligarh Muslim University, Aligarh, India
[20] Department of Physics, Ohio State University, Columbus, Ohio, United States
[21] Department of Physics, Sejong University, Seoul, South Korea
[22] Department of Physics, University of Oslo, Oslo, Norway
[23] Dipartimento di Elettrotecnica ed Elettronica del Politecnico, Bari, Italy
[24] Dipartimento di Fisica dell'Università 'La Sapienza' and Sezione INFN Rome, Italy
[25] Dipartimento di Fisica dell'Università and Sezione INFN, Cagliari, Italy
[26] Dipartimento di Fisica dell'Università and Sezione INFN, Trieste, Italy
[27] Dipartimento di Fisica dell'Università and Sezione INFN, Turin, Italy
[28] Dipartimento di Fisica e Astronomia dell'Università and Sezione INFN, Bologna, Italy
[29] Dipartimento di Fisica e Astronomia dell'Università and Sezione INFN, Catania, Italy
[30] Dipartimento di Fisica e Astronomia dell'Università and Sezione INFN, Padova, Italy
[31] Dipartimento di Fisica 'E.R. Caianiello' dell'Università and Gruppo Collegato INFN, Salerno, Italy
[32] Dipartimento di Scienze e Innovazione Tecnologica dell'Università del Piemonte Orientale and Gruppo Collegato INFN, Alessandria, Italy
[33] Dipartimento Interateneo di Fisica 'M. Merlin' and Sezione INFN, Bari, Italy
[34] Division of Experimental High Energy Physics, University of Lund, Lund, Sweden
[35] Eberhard Karls Universität Tübingen, Tübingen, Germany
[36] European Organization for Nuclear Research (CERN), Geneva, Switzerland
[37] Excellence Cluster Universe, Technische Universität München, Munich, Germany
[38] Faculty of Engineering, Bergen University College, Bergen, Norway
[39] Faculty of Mathematics, Physics and Informatics, Comenius University, Bratislava, Slovakia
[40] Faculty of Nuclear Sciences and Physical Engineering, Czech Technical University in Prague, Prague, Czech Republic
[41] Faculty of Science, P.J. Šafárik University, Košice, Slovakia
[42] Faculty of Technology, Buskerud and Vestfold University College, Vestfold, Norway
[43] Frankfurt Institute for Advanced Studies, Johann Wolfgang Goethe-Universität Frankfurt, Frankfurt, Germany
[44] Gangneung-Wonju National University, Gangneung, South Korea
[45] Gauhati University, Department of Physics, Guwahati, India
[46] Helsinki Institute of Physics (HIP), Helsinki, Finland
[47] Hiroshima University, Hiroshima, Japan
[48] Indian Institute of Technology Bombay (IIT), Mumbai, India
[49] Indian Institute of Technology Indore, Indore (IITI), India
[50] Inha University, Incheon, South Korea
[51] Institut de Physique Nucléaire d'Orsay (IPNO), Université Paris-Sud, CNRS-IN2P3, Orsay, France
[52] Institut für Informatik, Johann Wolfgang Goethe-Universität Frankfurt, Frankfurt, Germany
[53] Institut für Kernphysik, Johann Wolfgang Goethe-Universität Frankfurt, Frankfurt, Germany
[54] Institut für Kernphysik, Westfälische Wilhelms-Universität Münster, Münster, Germany
[55] Institut Pluridisciplinaire Hubert Curien (IPHC), Université de Strasbourg, CNRS-IN2P3, Strasbourg, France
[56] Institute for Nuclear Research, Academy of Sciences, Moscow, Russia
[57] Institute for Subatomic Physics of Utrecht University, Utrecht, Netherlands
[58] Institute for Theoretical and Experimental Physics, Moscow, Russia
[59] Institute of Experimental Physics, Slovak Academy of Sciences, Košice, Slovakia
[60] Institute of Physics, Academy of Sciences of the Czech Republic, Prague, Czech Republic
[61] Institute of Physics, Bhubaneswar, India

[62] *Institute of Space Science (ISS), Bucharest, Romania*
[63] *Instituto de Ciencias Nucleares, Universidad Nacional Autónoma de México, Mexico City, Mexico*
[64] *Instituto de Física, Universidad Nacional Autónoma de México, Mexico City, Mexico*
[65] *iThemba LABS, National Research Foundation, Somerset West, South Africa*
[66] *Joint Institute for Nuclear Research (JINR), Dubna, Russia*
[67] *Konkuk University, Seoul, South Korea*
[68] *Korea Institute of Science and Technology Information, Daejeon, South Korea*
[69] *KTO Karatay University, Konya, Turkey*
[70] *Laboratoire de Physique Corpusculaire (LPC), Clermont Université, Université Blaise Pascal, CNRS–IN2P3, Clermont-Ferrand, France*
[71] *Laboratoire de Physique Subatomique et de Cosmologie, Université Grenoble-Alpes, CNRS-IN2P3, Grenoble, France*
[72] *Laboratori Nazionali di Frascati, INFN, Frascati, Italy*
[73] *Laboratori Nazionali di Legnaro, INFN, Legnaro, Italy*
[74] *Lawrence Berkeley National Laboratory, Berkeley, California, United States*
[75] *Lawrence Livermore National Laboratory, Livermore, California, United States*
[76] *Moscow Engineering Physics Institute, Moscow, Russia*
[77] *National Centre for Nuclear Studies, Warsaw, Poland*
[78] *National Institute for Physics and Nuclear Engineering, Bucharest, Romania*
[79] *National Institute of Science Education and Research, Bhubaneswar, India*
[80] *Niels Bohr Institute, University of Copenhagen, Copenhagen, Denmark*
[81] *Nikhef, National Institute for Subatomic Physics, Amsterdam, Netherlands*
[82] *Nuclear Physics Group, STFC Daresbury Laboratory, Daresbury, United Kingdom*
[83] *Nuclear Physics Institute, Academy of Sciences of the Czech Republic, Řež u Prahy, Czech Republic*
[84] *Oak Ridge National Laboratory, Oak Ridge, Tennessee, United States*
[85] *Petersburg Nuclear Physics Institute, Gatchina, Russia*
[86] *Physics Department, Creighton University, Omaha, Nebraska, United States*
[87] *Physics Department, Panjab University, Chandigarh, India*
[88] *Physics Department, University of Athens, Athens, Greece*
[89] *Physics Department, University of Cape Town, Cape Town, South Africa*
[90] *Physics Department, University of Jammu, Jammu, India*
[91] *Physics Department, University of Rajasthan, Jaipur, India*
[92] *Physik Department, Technische Universität München, Munich, Germany*
[93] *Physikalisches Institut, Ruprecht-Karls-Universität Heidelberg, Heidelberg, Germany*
[94] *Politecnico di Torino, Turin, Italy*
[95] *Purdue University, West Lafayette, Indiana, United States*
[96] *Pusan National University, Pusan, South Korea*
[97] *Research Division and ExtreMe Matter Institute EMMI, GSI Helmholtzzentrum für Schwerionenforschung, Darmstadt, Germany*
[98] *Rudjer Bošković Institute, Zagreb, Croatia*
[99] *Russian Federal Nuclear Center (VNIIEF), Sarov, Russia*
[100] *Russian Research Centre Kurchatov Institute, Moscow, Russia*
[101] *Saha Institute of Nuclear Physics, Kolkata, India*
[102] *School of Physics and Astronomy, University of Birmingham, Birmingham, United Kingdom*
[103] *Sección Física, Departamento de Ciencias, Pontificia Universidad Católica del Perú, Lima, Peru*
[104] *Sezione INFN, Bari, Italy*
[105] *Sezione INFN, Bologna, Italy*
[106] *Sezione INFN, Cagliari, Italy*
[107] *Sezione INFN, Catania, Italy*
[108] *Sezione INFN, Padova, Italy*
[109] *Sezione INFN, Rome, Italy*
[110] *Sezione INFN, Trieste, Italy*

[111] *Sezione INFN, Turin, Italy*
[112] *SSC IHEP of NRC Kurchatov institute, Protvino, Russia*
[113] *SUBATECH, Ecole des Mines de Nantes, Université de Nantes, CNRS-IN2P3, Nantes, France*
[114] *Suranaree University of Technology, Nakhon Ratchasima, Thailand*
[115] *Technical University of Košice, Košice, Slovakia*
[116] *Technical University of Split FESB, Split, Croatia*
[117] *The Henryk Niewodniczanski Institute of Nuclear Physics, Polish Academy of Sciences, Cracow, Poland*
[118] *The University of Texas at Austin, Physics Department, Austin, Texas, USA*
[119] *Universidad Autónoma de Sinaloa, Culiacán, Mexico*
[120] *Universidade de São Paulo (USP), São Paulo, Brazil*
[121] *Universidade Estadual de Campinas (UNICAMP), Campinas, Brazil*
[122] *University of Houston, Houston, Texas, United States*
[123] *University of Jyväskylä, Jyväskylä, Finland*
[124] *University of Liverpool, Liverpool, United Kingdom*
[125] *University of Tennessee, Knoxville, Tennessee, United States*
[126] *University of the Witwatersrand, Johannesburg, South Africa*
[127] *University of Tokyo, Tokyo, Japan*
[128] *University of Tsukuba, Tsukuba, Japan*
[129] *University of Zagreb, Zagreb, Croatia*
[130] *Université de Lyon, Université Lyon 1, CNRS/IN2P3, IPN-Lyon, Villeurbanne, France*
[131] *V. Fock Institute for Physics, St. Petersburg State University, St. Petersburg, Russia*
[132] *Variable Energy Cyclotron Centre, Kolkata, India*
[133] *Vinča Institute of Nuclear Sciences, Belgrade, Serbia*
[134] *Warsaw University of Technology, Warsaw, Poland*
[135] *Wayne State University, Detroit, Michigan, United States*
[136] *Wigner Research Centre for Physics, Hungarian Academy of Sciences, Budapest, Hungary*
[137] *Yale University, New Haven, Connecticut, United States*
[138] *Yonsei University, Seoul, South Korea*
[139] *Zentrum für Technologietransfer und Telekommunikation (ZTT), Fachhochschule Worms, Worms, Germany*

JHEP07(2015)051